CLEAN PLATINUM NANO-CATALYSTS MADE EASY

by

Qiudi Meng

B.E. Chemical Engineering, Jiangnan University, 2016

Submitted to the Graduate Faculty of

the Swanson School of Engineering in partial fulfillment

of the requirements for the degree of

Master of Science

University of Pittsburgh

2019

UNIVERSITY OF PITTSBURGH

SWANSON SCHOOL OF ENGINEERING

This thesis was presented

by

Qiudi Meng

It was defended on

March 26 2019

and approved by

Dr. James R. McKone, Ph.D., Assistant Professor
Department of Chemical and Petroleum Engineering

Dr. Susan Fullerton, Ph.D., Assistant Professor
Department of Chemical and Petroleum Engineering

Dr. Robert Enick, Ph.D., Professor
Department of Chemical and Petroleum Engineering

Thesis Advisor: Dr. James R. McKone, Ph.D., Assistant Professor
Department of Chemical and Petroleum Engineering

CLEAN PLATINUM NANO-CATALYSTS MADE EASY

Qiudi Meng, M.S.

University of Pittsburgh, 2019

Platinum is widely used in electrochemical and gas-phase catalysis due to its excellent stability and high activity toward a range of important reactions. Thus, Pt is also often used to benchmark the activity of other catalysts, especially in electrocatalytic processes involving hydrogen and oxygen[1, 2]. The electrochemical behavior of platinum nanoparticles has been of great interest for many research groups working on fuel cells for a long time. Hence, there are many papers reviewing the size and electrochemical properties of platinum nanocatalysts [3, 4, 5, 6, 7]. In those context, several methods have been reported for the preparation of monodisperse Pt nanoparticles whose surfaces are essentially free of contaminants. However, these methods are difficult to implement in an engineering laboratory with limited facilities and expertise for wet chemical synthesis.

We have developed a synthetic procedure for catalytically active Pt nanoparticles that uses only readily available tools and reagents at high safety level, with the goal of making high-quality control experiments in electrocatalysis as easy as possible. Our procedure is based on reduction of aqueous Pt(IV) salts by ascorbic acid in the presence of a polyacrylate capping agent, which can then be removed using a base treatment and a series of solvent washing steps. Our results show that this method produces a high yield (60%) of 3–4 nm particles exhibiting the characteristic features of clean Pt surfaces in cyclic voltammetry that is comparable to commercial nanoscale platinum catalysts. These nanoparticles also perform well in catalyzing hydrogen evolution and oxidation experiments in a 3-electrode system.

Table of Contents

List of Tables

List of Figures

Preface

The basis for this research originally stemmed from my passion for developing better understanding of catalysis and electrochemistry. In truth, I could not have achieved my current level without a strong support group. First of all, my advisor James McKone, who provided patient advice and guidance during all my Master study. And secondly, my group members, each of whom has supported me with kindness, help and understanding throughout the research process. I would like to especially thank Patil, Rituja Bhagwant, Hoffmann, Jeffrey O, and Deng, Yifan for reviewing my thesis and providing unwavering support to my research.

1.0 Introduction

1.1 Purpose And Scope

This thesis presents in some detail the entirety of the work that I have pursued over the last year through my involvement with the McKone group at Pitt. It has been written in part to satisfy the requirements for a Master's degree in chemical engineering from University of Pittsburgh. Chapter-1 presents a general overview of the field of water electrolysis, fuel cells and hydrogen production based on the understanding I have developed during this work. It focuses primarily on acidic hydrogen evolution systems, along with a brief introduction to catalyzing these reactions. The thesis continues in Chapter-2 with a thorough description of the development of a fresh synthetic scheme for producing unsupported platinum nanoparticles along with the experimental and material synthetic techniques and purification steps that were learned and employed during the course of this work. Several detailed measurement and characterization studies are also included. Chapter-3 provides our evaluation of the size/shape, yield, and electrochemical catalytic activity of the synthesized Pt catalysts. It also covers the significance of the purification process methods along with comparison to commercial catalysts. The next chapter, Chapter-4, presents electrochemical experiments such as hydrogen evolution and oxidation reactions and open circuit potential measurements with our catalysts. This is provided to allow for a better interpretation of the results presented and to give a more visualized understanding of the activity of catalysts as synthesized. Finally, Chapter-5, is a summary of my work along with my suggestions towards the potential directions for future work of this project.

I hope that this work will help enhance our understanding of platinum nanocatalysts and of HER/HOR catalysis in general and open sufficient avenues for further work on these systems that might extend to meeting our long term goal of designing practical electrolyzers and fuel cells.

1.2 Hydrogen Fuel Cells

A hydrogen fuel cell is an energy transfer system that is widely used nowadays. The working mechanism can be simply described as the reaction between hydrogen and oxygen to become water, where electrical energy is produced during the process[8]. Figure 1.1 shows a schematic image of a hydrogen fuel cell using a proton-conducting electrolyte.

At the anode, hydrogen fuel is inserted into the cell and is converted to protons and electrons. The cathode uses the electrons produced by the anode to react with oxygen and the protons to become water. In an alkaline environment (Figure 1.2) the hydrogen fuel is still applied to the anode side, reacting with OH^- and form water and electrons. At the cathode side, oxygen from air reacts with the electrons and water to become OH^-.

As it can be seen from Figures 1.1 and 1.2, no matter what the electrolyte is, the electrolyte in the middle of the cathode and anode can only let the H^+ or OH^- pass through it, but not the electrons. The electrons must pass through the external electric circuit and can be used as electric power.

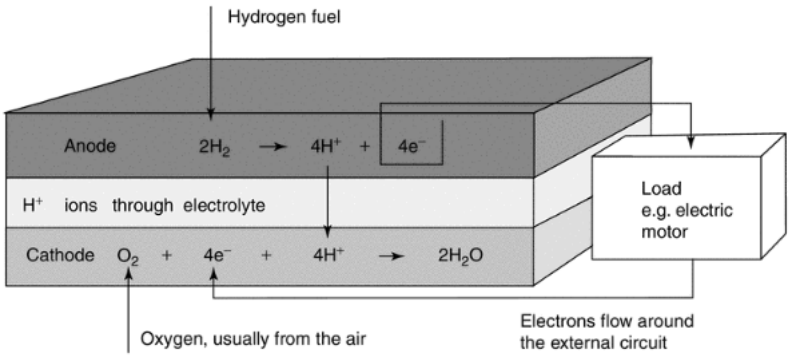

Figure 1.1: Electrodes reactions and electron flow in an acid electrolyte fuel cell [8]. Figure reprinted with permission from James L et al. Fuel Cell Systems Explained, 3rd Edition, Jul 2018, Pages7. Copyright 2018 by John Wiley and Sons.

Two major problems with fuel cells are as follows:

1. The low reaction rate usually leads to small electric current and low power in fuel cell system. Increasing actual reaction rate is one of the focuses to enable fuel cell as a better power transfer technique in practice.

2. The fuel cell uses hydrogen as fuel, but hydrogen is not readily available or pure enough now that it can not be applied to fuel cells for direct use. More advanced methods to produce high level purified hydrogen need to be introduced to provide qualified power resource.

Various types of fuel cells have been designed to solve these problems in different ways such as alkaline fuel cells, proton exchange membrane fuel cells, direct methanol fuel cells, phosphoric acid fuel cells and so on. The main focus of this thesis is on platinum catalysts, which are used primarily in two types of fuel cells—the polymer exchange membrane fuel cell (PEMFC) and alkaline fuel cell (AFC).

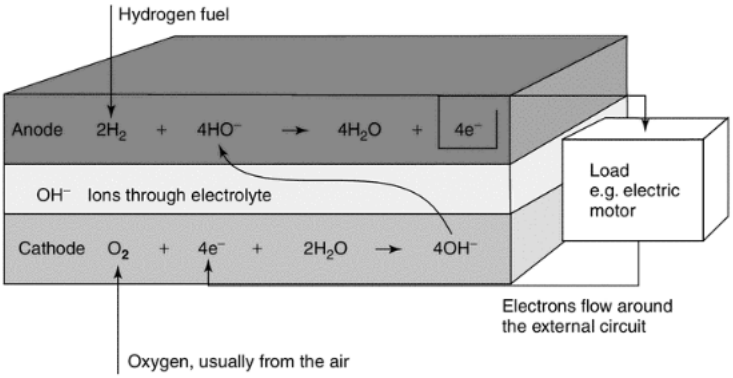

Figure 1.2: Electrode reactions and electron flow direction in the base electrolyte fuel cell [8]. Figure reprinted with permission from James L et al. Fuel Cell Systems Explained, 3rd Edition, Jul 2018, Pages 8. Copyright 2018 by John Wiley and Sons.

1.3 Hydrogen and Water Electrolysis

Hydrogen is widely used not only as an energy storage system for fuel cells as mentioned in last section, but in other applications such as in petroleum and gasoline refining [9], ammonia production and methanol synthesis[10], and metal refining such as with nickel, copper, tungsten, molybdenum, zinc and uranium[11]. The large size of these industries requires large scale hydrogen production. But the main challenge is, as mentioned earlier in last chapter, the availability of hydrogen fuel. One of the best methods for making hydrogen is by water electrolysis because water is quite an abundant resource, and electrolysis has become a mature industry for producing hydrogen. Although water electrolysis has the advantage of simplicity and has been known for over 200 years [12, 13], it has several challenges for widespread use and only accounts for around 4% of the world's hydrogen production. The main reasons for this include: high energy consumption, high cost and maintenance compared to fossil-fuel based hydrogen production methods, and low reliability, durability and safety[14]. Currently hydrogen production for marine uses, spacecraft, the electronic industry, and the food industry[15] relies mainly on the reforming of natural gas[16].

Water electrolysis can be seen as the reverse process of a working hydrogen fuel cell. The reactions on each electrode is discussed below, taking the acid electrolyte as an example.

$$\text{Anode: } 2\,H_2O \longrightarrow O_2 + 4\,H^+ + 4\,e^- \tag{1.1}$$

$$\text{Cathode: } 4\,e^- + 4\,H^+ \longrightarrow 2\,H_2 \tag{1.2}$$

$$\text{Overall: } 2\,H_2O \longrightarrow O_2 + H_2 \tag{1.3}$$

The device also closely resembles a fuel cell where the main differences are (a) the voltage applied and (b) the direction of current and ion flow. Still take acid atmosphere as an example, when the reaction begins, electrons flow from the anode to cathode through outer electric motor. In order to keep the electrical charge as a balance, protons produced by anode also transfer to cathode, where protons at cathode consume electrons and form hydrogen. In order to enhance the conductivity of the solution, electrolytes consisting of high mobile ions are used[17]. Sodium hydroxide or potassium hydroxide are most commonly used because they can avoid the huge corrosion loss in acid electrolytes[18]. A highly active and stable electrode is also used in electrolysis to increase efficiency. By the use of a diaphragm or membrane, gas receivers can collect hydrogen and oxygen generated during the process of water electrolysis.

Water electrolysis can play an important role in a renewable energy production, conversion, storage and use system. Figure 1.3 shows how hydrogen can act as an energy storage in a conceptual distributed system and can act as fuel[14]. When the solar energy from sun comes to be used in water electrolysis, hydrogen was produced. Then the hydrogen can either act as an energy storage for future use in fuel cell, or be used directly after produced as a fuel gas.

When abundant renewable energy is available, excess energy could be stored as hydrogen by water electrolysis and then used in fuel cells to generate electricity. A number of studies have reported renewable energy sources such as solar or wind energy [19, 20, 21]. Those energies can be transferred by water electrolysis to hydrogen. The whole procedure is like a cycle and hydrogen acts inside as a media to change excess energy to the electricity that people can use.

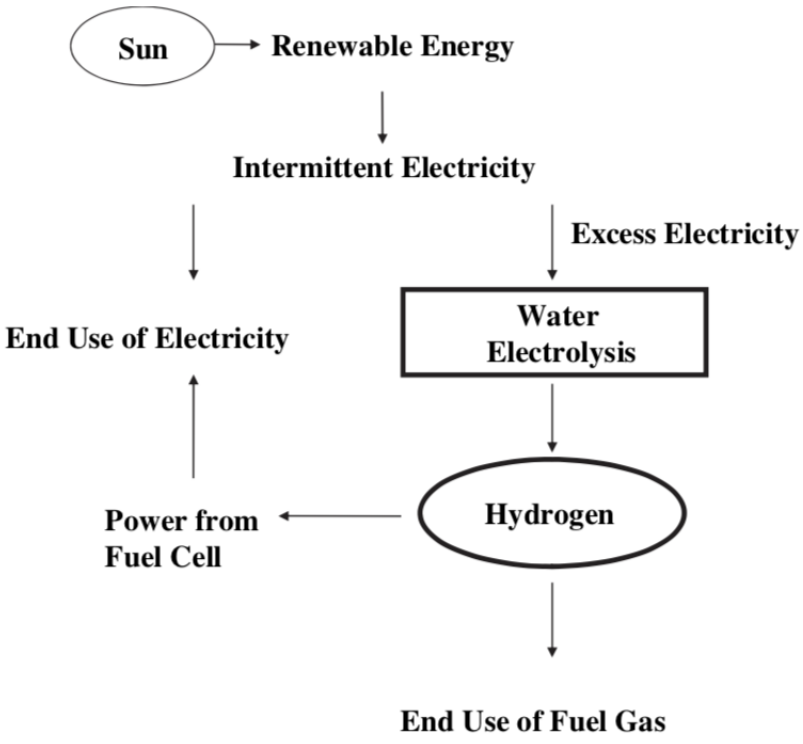

Figure 1.3: Importance of hydrogen in conceptual energy storage system and its mechanism [14]. Figure reprinted with permission from Zeng et al., Progress in Energy and Combustion Science, Volume 37, Issue 5, September 2011, Pages 631. Copyright 2010 by Elsevier.

1.4 Platinum Catalysts

Catalysts accelerate chemical reactions, enabling us to operate chemical processes at lower temperatures and pressure. Since the 1960s, heterogeneous catalysis has assumed a star role to be one of the most promising and fastest growing technologies for the chemistry field. The importance of catalytic technology and the impact on our life and society make catalytic production of chemicals and fuels an important aspect of the whole economy, as well as a fundamental part of our life.

There are three major areas of catalyst technology: chemical production, petroleum refining, and environmental clean-up [22]. Representative catalysts and reactions are listed in table1.1.

Table 1.1: Representative catalysts and reactions. Adapted from James L et al. [8].

Item name	Example	Reaction synthesized
Metals	Fe, Co, Ni, Cu, Ru, Pt, Pd, Ir, Rh, Au	Hydrogen, steam reforming, HC reforming, dehydrogenation, ammonia synthesis, Fisher-Tropsch synthesis
Oxides	Oxides of V, Mn, Fe, Cu, Mo, Al, Si, Sn, Pb, B	Complete and partial oxidation of hydrocarbons and CO, acid-catalysed reactions, methanol synthesis
Sulfides	Sulfides of Co, Mo, W, Ni	Hydrotreating, hydrogenation
Carbides	Carbides of Fe, Mo, W	Hydrogenation, FT synthesis

If a catalyst is to be commercially useful, it must be active, selective, and robust[23]. The cost should be also reasonable and acceptable according to the number of products the catalyst produces. Stirring or agitation is often used in most reactions to improve the uniformity of the reaction, which requires the catalyst must be mechanically strong enough to avoid degradation.

Platinum is precious and rare, but widely used across many sectors and has grown to be the 3rd most heavily traded metal in the world[24]. In electrochemistry, Pt is the most

commonly used metal catalyst for fuel cell application because it exhibits high activity toward a range of important reactions[25, 22]. In addition, although Pt is one of the most reactive metals, it is resistant to oxidation or corrosion during the reaction, which is why we say it is stable.

The usage of platinum is incredibly wide in catalytic application: multi-phase laboratory catalyst, electrodes for fuel cells, thermometers[26], etc. Platinum's resistance to corrosion is especially useful for electrochemical processes, such as electrowinning of copper and zinc, waste water treatment and harsh organic reactions such as electrochemical fluorination[27]. Figure 1.4 illustrates the structure of active sites of a catalyst nanoparticle.

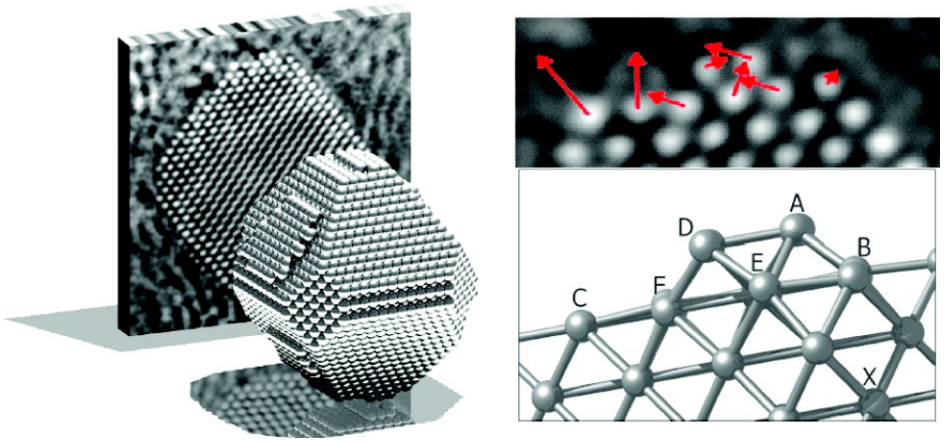

Figure 1.4: Platinum nanoparticle active sites. Figure reprinted with permission from Chang et al., Nano Lett. 2010, 10, 8, 3073-3076. Copyright 2010 by American Chemical Society.

The left panel shows that a platinum particle may expose multiple tangent planes as different crystal facets. The right panel shows various active sites that can adsorb and desorb reactants. According to Chang et al [28], based on comparison between experimental and theoretical atomic structures of Pt surface, the surface platinum atoms can move when the reactant is close to Pt surface. When the surface platinum atoms move, platinum atoms underneath the surface may become exposed to reaction. More surface or active sites enhance more bonds to be produced at the same time, leading to faster reaction rate.

There are still challenges for using Pt as a catalyst, although it is so good at hydrogen electrochemistry. The most important challenge is its high price, which requires metal control

and recovery to avoid the loss of catalyst material[29]. One possible solution for this problem is to create a higher surface area of catalyst by making them small enough in size , because This ensures utilizing small amount of Pt to yield maximum activity.. This physical property is also required by commercial catalyst to reach the higher activity standard. To increase the surface area, porous catalysts or smaller size catalysts are always used to induce the large surface area per unit mass. In order to reduce the size, people change bulk catalysts into particles, and then making the particles into smaller ones. Nanometer-sized catalysts become very prominent in fundamental and applied surface science nowadays because they will improve the reactivity a lot with less amount in experiment[30]. The actual catalytic efficiency of nano particles depends on the electronic interaction between the catalysts and the reactant molecules and also the surface-volume ratio[31]. Some researchers even hold the idea that for particle sizes of 100nm or lower, surface effects become more important than material properties [32].

The properties of Pt nanoparticles have been the subject and interest of various studies in both catalysis and electrochemistry field, not only because of the important role this catalyst plays in practical electrodes, but also because it helps better understand the properties influenced by the structure and size of the crystals in electrochemistry[33]. However, because Pt is so high in cost, many catalysts made of more abundant, inexpensive, multi-phase or porous structure are being researched [34, 35, 36]. Nonetheless, Pt is often used to benchmark the activity of these other catalysts, especially in electrocatalytic processes involving hydrogen and oxygen.

Several methods have recently been reported for the preparation of monodisperse Pt nanoparticles whose surfaces are essentially free of contaminants. However, these methods are difficult to implement in an engineering laboratory with limited facilities and expertise for wet chemical synthesis [37]. The aim of this work was to develop a synthetic procedure for a novel platinum nanoparticle that is simple and reproducible with only readily available tools and reagents. The clean platinum nanoparticles possess large surface area and uniform size distribution with the goal of making high-quality control experiments in electrocatalysis as easy as possible.

2.0 Experimental

2.1 Catalyst Synthesis

The following describes in detail a representative Pt nanoparticle synthesis based on an optimized procedure adapted from Ahamadi et al.[38]. These nanoparticles are synthesized by reduction of aqueous H_2PtCl_6 in the presence of polyacrylate and ascorbic acid. Polyacrylate acts as the capping agent, which covers the nanoparticle surfaces as they grow. Ascorbic acid is the reducing agent that will convert the soluble salt to Pt metal. The chemicals used are all of analytical grade and purchased from commercial sources. The water used in the experiment is purified to $\geq$18 MΩ cm resisitivity using a Millipore water purication system.

Before each synthesis process, an ascorbic acid stock solution is prepared by adding 0.195g ascorbic acid (Alfa Aesar, 99.5%) to 10mL of water. A new stock solution needs to be prepared every time because ascorbic acid is not indefinitely stable in water. Its aqueous solution was reported to be oxidized by air over 1-2 days in water[39]. Also based on our own experience, fresh ascorbic acid will turn yellow after several days and can no longer reduce the platinum salt successfully.

Next, a 100mM aqueous polyacrylate (PA, Alfa Aesar, 99.5%) stock solution is mixed and sonicated for 5 min. Then the a stock solution was made with 12 mM concentration of H_2PtCl_6 in water (Alfa Aesar, 99.5%). For each sample, 0.833g of the platinum salt solution, 1 mL of the ascorbic acid stock solution, and 0.1 g of the polyacrylate stock solution are mixed with water to make an 10 ml aqueous solution in a 20ml glass vial. The appearance of this mixture is initially transparent with yellowish colour. A small stir bar is put into the mixture, and a silicone oil bath is preheated on a hotplate to 90°C. Once the temperature stabilizes, the precursor is put into the oil bath and heated for 60 min while stirring at 600rpm. A thermometer is inserted into the precursor to ensure the temperature is always stable within a $\pm$3 degree range. The solution turns black and opaque in around 15 min after being put into the bath oil, as shown in Figure 2.1, indicating platinum particles are reduced successfully from the salt. As the colloidal mixture is heated for 60 min continuously

at near boiling temperature, the solution tends to lose water over time. In order to avoid the changes caused by water evaporation, additional water is added every 20 min to maintain a constant reactant concentration.

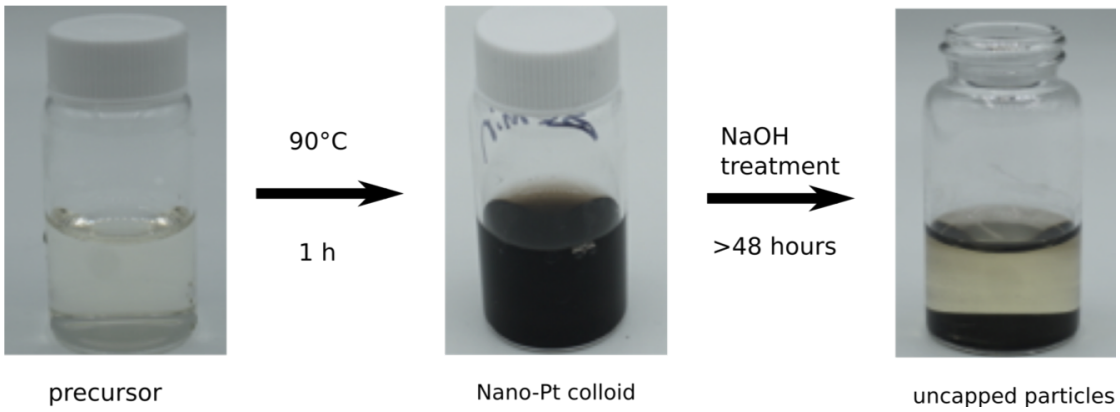

Figure 2.1: Pt catalyst synthesis from precursor to uncapped, clean particles.

After 1 hour of synthesis, the glass vial was removed from heat and left to cool down to room temperature. A pellet of sodium hydroxide (around 0.2 g in mass) was then put into the suspension after it cooled down completely at room temperature. After waiting for at least 24 hours, the particles separated from the supernatant by settling to the bottom of the vial, as shown in figure 2.1. Most of the supernatant was then removed using a pipette. 5 mL of isopropanol alcohol (IPA) was then added to the suspension to improve separation upon centrifugation.

The vial is then sonicated in order to let Pt particles suspended in the new solvent homogeneously. After sonication, the suspension is divided into several 2 mL centrifuge tubes. These samples are centrifuged at 10,000 rpm for 5 min, 3 times in total. Between each centrifuge step, the supernatant is removed and refilled with water and IPA at a 1:4 ratio, and then the tubes are sonicated for 1 min until all the sediment disappears. After the purification is complete, the particles are suspended in pure water in a clean centrifuge tube.

2.2 Reaction Schemes

Figure 2.2 depicts the postulated reaction by which Pt^{4+} is reduced to Pt^0 by ascorbic acid. The Pt is initially solubilized by coordination to six chloride ions, and the overall charge on the compound is compensated by two protons (H_2PtCl_6). Ascorbic acid can be oxidized to form dehydroascorbic acid, which involves loss of two protons and electrons. Therefore, upon reaction with two equivalents of ascorbic acid, the Pt^{4+} gains four electrons to generate Pt^0, whereupon it sheds its chloride ligands to generate six equivalents of HCl.

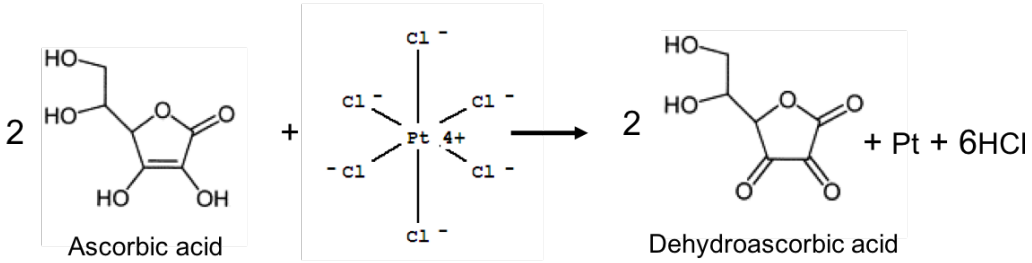

Figure 2.2: Proposed scheme for the reaction between ascorbic and platinum(IV) to obtain Pt nanoparticles [40]. Figure reprinted with permission from Fayle et al., Food Chemistry, Volume 70, Issue 2, August 2000, page 193. Copyright 2000 by Elsevier.

Figure 2.3 depicts a proposed scheme by which Pt generates soluble nanoparticles upon reduction in the presence of polyacrylate as well as the removal of polyacrylate via base treatment. The first step in particle formation is the formation of Pt nuclei (generally less

than 1 nm in diameter). We propose that these nuclei contain partially reduced Pt species that retain a positive charge, which can therefore be stabilized by the negatively charged carboxylates on the polymer.

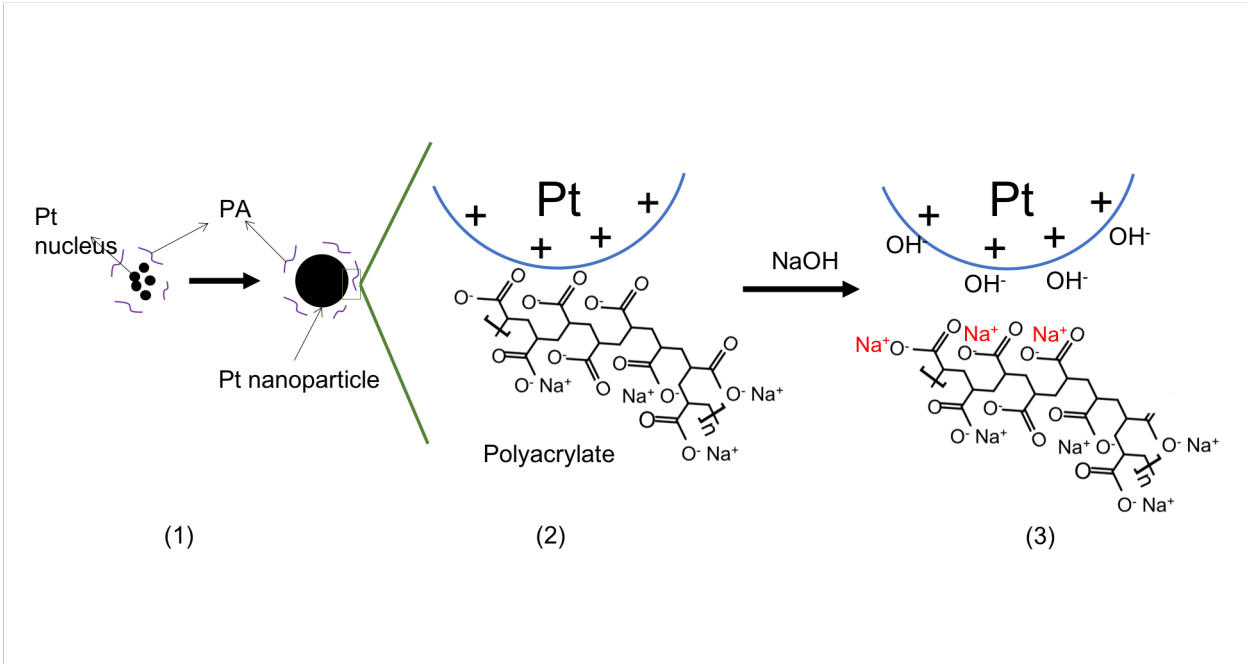

Figure 2.3: Scheme depicting the capping of Pt nanoparticles by sodium polyacrylate (1–2) and de-capping due to the addition of NaOH (3).

Further coalescence and growth of the nuclei into nanoparticles results in continued strong coordination of the polyacrylate polymer to the surface, either due to a continued net positive charge on the surface of the particle and/or the chelating behavior of the polyacrylate. Because every charged group on the polyacrylate is unlikely to be strongly bound to the Pt, the remaining charged species can interact favorably with the water environment to keep the Pt nanoparticles soluble.

Removal of the polyacrylate from the Pt nanoparticles via the base treatment could occur by either of two processes. First, the base could catalytically depolymerize the polyacrylate, thereby reducing its ability to stabilize the particles. However, we do not believe this to be the case since increasing amounts of base above 0.35 M did not cause the nanoparticles to fall out of solution faster. Instead, we expect the base treatment introduces a large

excess of hydroxide to the solution (note that the polyacrylate is only present in a 1 mM concentration on a monomer basis), which preferentially binds to the positively charged Pt surface, causing it to shed its polyacrylate ligands. This greatly destabilizes the colloid, allowing the Pt particles to settle out of solution over the span of hours.

2.3 Yield measurement

The theoretical solid particle yield of reaction was calculated by dividing the actual mass by theoretical mass of the particle. Theoretical platinum mass in the product is calculated by multiplying the platinum concentration and molar mass. The actual mass of Pt nanoparticles was measured by depositing the nanoparticles on microscope slides and weighing the mass difference before and after sample deposition.

A microscope slide was cleaned and dried completely in air and weighed before the sample deposition. A known volume of suspended particles (already sonicated to reach homogeneous suspension) was deposited on the slide and allowed to dry completely in air until the nanoparticles formed a film. During the suspension drying process, sample converted from a flowing fluid to a dark solid shadow that had many layers and reflected light when changing the direction exposed to light, indicating that a nanoparticle film had been formed. The film was transparent first and became opaque when the deposition increased. Then the slide was weighed again and the difference was taken as the weight of platinum nanoparticles. To avoid the possibility of excess mass from adsorbed water, the nanoparticle film was further dried under an infrared lamp in air for 10 min and weighed a third time.

2.4 Transmission Electron Microscopy (TEM)

The platinum nanoparticles are characterized on a transmission electron microscope (JEOLTEM 2100F) to assess their morphology and size. During TEM the composition of the sample is also measured using energy-dispersive spectroscopy (EDS). The TEM sample is

prepared using a copper-carbon TEM grid by taking a small amount of the sonicated original suspension and diluting it 10-fold. Then the diluted sample is sonicated again, and a drop or two of suspension is deposited onto the grid and dried completely in a 60 °C oven for 10 min.

2.5 Electrochemical Characterization

2.5.1 Electrode Preparation

Electrodes were prepared using Pt nanoparticle suspension deposited onto polished glassy carbon electrodes (hereafter nano-Pt/GC). Before the deposition, a 3mm diameter glassy carbon electrode was first polished on 10μm, 5μm, and 1μm alumina powder in order and with polishing paper. For each size powder the electrode was polished 20 cycles clockwise and then 20 cycles in anticlockwise direction. After the polishing procedure, the glassy carbon electrode was washed with pure water to remove the alumina powder. The platinum nanoparticles were diluted, sonicated to suspend, and deposited on the glassy carbon electrode at a known mass concentration under the assumption of unit particle yield.

2.5.2 Hydrogen Adsorption and Desorption

A cyclic voltammetry plot with clear hydrogen adsorption and desorption peaks helps show if there are clean platinum surface area in the sample that can address the reaction. Furthermore, the peaks in CV plots can also be used to mathemetically calculate how much active surface area the sample exposes to reaction. A three-electrode electrochemical cell was setup with an Ag/AgCl reference electrode, a nano-Pt/GC working electrode, and Pt wire as counter electrode to determine the hydrogen bond breaking and forming characteristics of Pt particles. A Gamry Reference 600+ Potentiostat was attached to this setup as the power source and current measuring system. The experiment was run in 0.5 M aqueous sulfuric acid electrolyte. The electrolyte was continuously purged with nitrogen for 20 min before the electrochemical measurement in order to remove all the oxygen.And the nitrogen purge

was lifted to the surface of electrolyte when CV was running to avoid the disturbance to plots and peaks. Electrochemical cleaning step was employed before collecting actual CV data. A cyclic voltammetry (CV) was run from -0.4 to 1.4 V vs Ag/AgCl at a 100mV/s scan rate for 3 cycles as a cleaning step. Experimental data was then collected using CV from -0.25 to 1.25 V vs Ag/AgCl at 100 mV/s.

Control measurements using a flat Pt "button" electrode were made before and after the nanoparticle electrode CV to ensure the electrolyte was stable. The reversible hydrogen electrode potential (RHE) was also determined after experimentation by measuring the open circuit potential (OCP) of a clean Pt electrode in the same cell setup. Nitrogen was first purged into the cell for 20 min before measuring to remove oxygen completely. Then OCP experiment started with nitrogen still purging into the electrolyte. After 60 sec, the nitrogen purge was changed to hydrogen purge, causing the potential to rapidly shift negative. The measurement continued until the potential variation range was within 5mV over 120 sec, at which point the OCP is recorded as 0 V vs RHE.

2.5.3 Comparison with a Commercial Catalyst

In order to see how effective our Pt nanoparticles are toward electrocatalytic reactions, we compared our sample with commercial Pt deposited on carbon black (hereafter Pt/C). A colloid with the same concentration of Pt (0.2g/mL) was made according to a literature report[41] and finally suspended in water. This solution is then used to prepare a Pt/C film on a glassy carbon electrode in the same way as with our Pt nanoparticles.

2.5.4 Hydrogen Evolution Reaction

We measured the catalytic activity of nano-Pt/GC toward the hydrogen evolution reaction (HER) in base and acid environments using the same 3-electrode system with a rotating working electrode. Before the experiment, hydrogen was purged for 20 min in order to remove oxygen and allow the electrolyte to saturate with hydrogen. After electrochemical cleaning using CV, the OCP is determined as described previously. Then the HER measurements are carried out over the scan limits from -350mV to 150 mV vs Ag/AgCl. Scan rates

and working electrode rotation speed were varied, as described in the results section below. After recording the raw data, the open circuit potential was substracted from the measured potential to convert to the RHE reference.

A post correction for uncompensated resistance is still needed to avoid the error before we export the data. Electrochemical test cells have multiple resistance caused by electrolyte and the wires. Current flow through solution resistance can cause significant errors in potential measurements. Some of the resistance can be compensated by putting the reference electrode in cell, but the reference electrode cannot be placed infinitely close to the working electrode or super small to completely reduce the resistance. There is always resistance left in the cell, which is uncompensated resistance (R_u), that needs to be counteracted before measurement. The value of R_u can be measured using a straightforward high frequency alternating-current technique and the data corrected for the overpotential associated with solution resistance. After those corrections the data were visualized using a Tafel plot to compare the current density of hydrogen evolution and oxidation.

3.0 Results and Discussion

3.1 Influence of Centrifugation Method

Before an efficient purification procedure was developed, the Pt particles were suspended in pure water before and between each centrifugation cycle. The supernatant was quite dark, especially after the first cycle, meaning that Pt particles could not be successfully separated even at the highest centrifuge speed (15,000 rpm) for 20 min. This needs to be fixed because Pt is too precious to be lost in the supernatant. Several changes were attempted to the centrifuge speed, time, and solvent mixture of the suspension, all in vain. Finally, a new centrifuge method that worked considerably better. It involved adding IPA together with water as the purification solvent. The comparison of purification results with only water and with this water/IPA mixture can be seen in Figure 3.1.

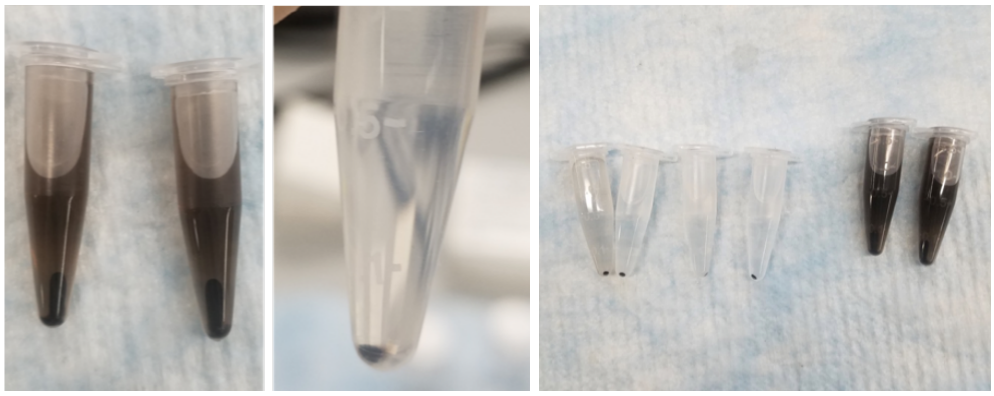

Figure 3.1: Left:sample after centrifuge with pure water as suspension; Middle: sample with IPA inside after centrifuge. Right: left 4 tubes are with IPA and water as suspension, right 2 tubes are pure water as suspension. All the 6 tubes are centrifuged at 10000 rpm for 10 min together.

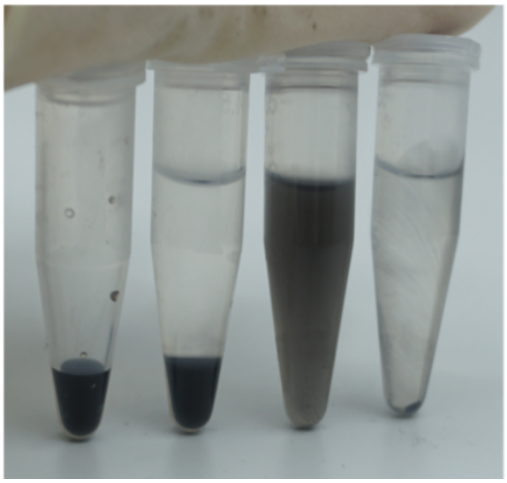

Figure 3.2: The far left tube: particles suspended well in water and became a homogeneous suspension; Second tube: IPA (upper transparent layer) is added to the tube and separate with water layer; The third tube: After sonication 2 solvents mix together;Last tube: After centrifuge the particles come down to the bottom again.

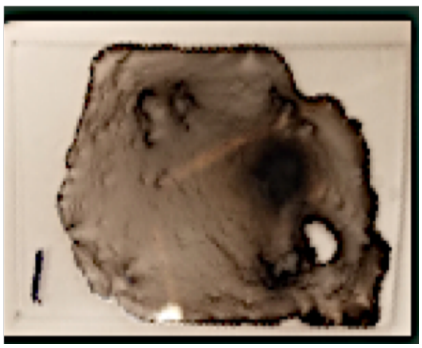

Figure 3.3: platinum catalysts are deposited on the microscope slide and then form a homogeneous film to measure the mass difference

Figure 3.2 shows the steps of the improved method. First, water is added to suspend the particles. Then IPA is added and sonicated to mix well. After centrifugation, the supernatant is quite clear with all the particles settling to the bottom. Adding IPA to the suspension not only makes the supernatant clearer, but also shortens the required centrifuge time and speed: 5 minutes at 8,000 rpm is chosen to be the optimal condition for centrifugation. The solvent mixture works best at 80%(volume fraction) IPA and 20% water after several control experiments. It is important to mention that water must be added first to the Pt nanoparticle pellet, and the tube needs sonication to suspend the particles from the bottom before IPA is added. If IPA comes into the tube first, the particles do not suspend well, so that the polyacrylate and ascorbic acid may not be removed completely.

3.1.1 Particle Yield

As mentioned in experimental part, particles actual mass was determined by measuring difference between and after sample deposition on slides. Figure 3.3 shows a Pt nanoparticle film deposited on a glass slide for a particle yield measurement. The measured yield of particles before and after drying is shown in table 3.1.

The yield of particles was about 67% after purification. We also compared the behavior of uncapped particles and capped particles that were not treated using base or electrochem-

ical methods. The comparison results show that base treatment does help to clean the nanoparticles, however the result may not be accurate enough to draw that conclusion. The particles weight is too small compared to the slides weight, and the microbalance we use to measure the weight is very delicate, which means even a tiny amount of dirt attached to the slide when we pick it up or drop it off will make a big difference. But the results indicate we have gotten a step closer to our goal–an easy and reproducible way to synthesize the catalyst, because higher yield compared to other papers is reached with very common organic solution.

Table 3.1: Mass difference and yield comparison between uncapped and capped nano particles

Item Name	Uncapped sample	Capped sample
slide weight (mg)	2173.315	2328.640
slide + sample (mg)	2173.447	2330.633
Actual particle weight (mg)	0.132	1.993
Theoretical weight (mg)	0.195	0.195
yield (%)	67.70	199.89
weight after heating (mg)	0.113	1.812
yield after heating (%)	57.94	181.74

3.2 Particle Size and Shape

Particle size and shape need to be known clearly to verify if nanoscale particles are synthesized successfully. Another purpose is to calculate theoretical surface area of nanoparticles in order to compare with electrochemical surface area the sample expose to reaction. TEM images of particles shown in Figure 3.4 show very homogeneous platinum particles of uniform size on the order of 3–4 nm in diameter. However, the particles are also strongly agglom-

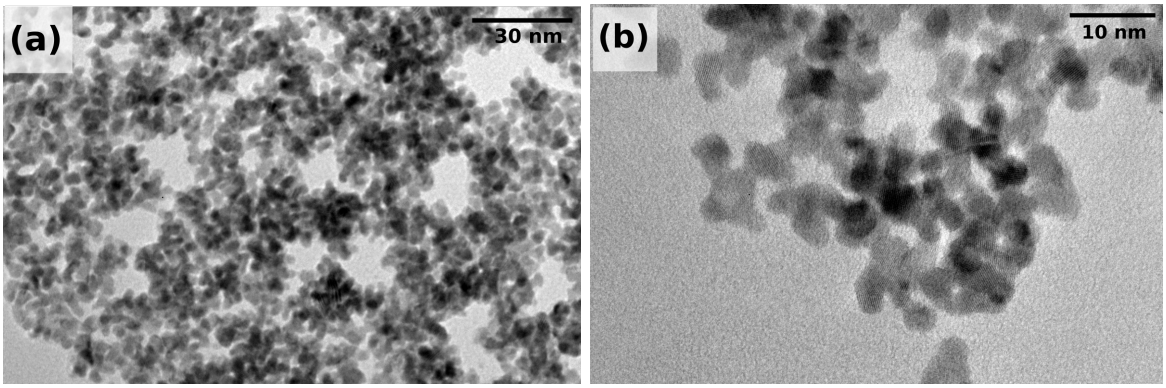

Figure 3.4: uniform size nanoparticles at 3-4 nm diameter were synthesized successfully in the experiment

erated, making less surface area exposed to the experiment. This problem is very common to the particles at such small sizes and needs to be solved by improving the synthesis or purification method in the future.

The composition of catalyst was also characterized using energy-dispersive x-ray spectroscopy (EDS) in the TEM. These results are shown in figure 3.5. The EDS elemental mapping shows that there are still sodium and carbon compounds in our particles, together with oxygen, although measuring oxygen in EDS is always difficult and inaccurate. The sodium left in our sample could be from the capping agent–sodium polyacralate, or from the base added after synthesis to remove capping agent.It is difficult to define what other impurities they are, but they must relate to ascorbic acid, IPA, or their side products during synthesis and purification.

Comparison experiments were also conducted on sample without sodium polyacrylate to see if Pt nanoparticles can be synthesized successfully without capping agent. If so, some impurities caused by PA could be removed from the sample and particles will become cleaner and give more surface areas. One synthesis mixture contained no PA and the second contained 1 mM PA. After synthesis at 90 °C for 1 hour, both of the samples turn dark in colour. The particles in the PA-free sample settled down to the bottom of the vial after a few

Element	At. No.	Line s.	Netto	Mass [%]	Mass Norm. [%]	Atom [%]
Sodium	11	K-Serie	2395	0.49	0.49	4.01
Platinum	78	K-Serie	129	99.51	99.51	95.99
			Sum	100.00	100.00	100.00

Element	At. No.	Line s.	Netto	Mass [%]	Mass Norm. [%]	Atom [%]
Sodium	11	K-Serie	4788	0.91	0.91	7.24
Platinum	78	K-Serie	137	99.09	99.09	92.76
			Sum	100.00	100.00	100.00

Figure 3.5: EDS results show our platinum composition is more than 99% for mass percentage and 94.38% for atom ratio.

hours after the synthesis, whereas the PA sample remained homogeneous after 12 hours until the centrifugation was conducted to purify the particles. TEM images of both samples, shown in Figure 3.6 suggest that the Pt crystal size isn't strongly influenced by the capping agent, but the extent to which they agglomerate is significantly influenced by capping agent. The 3–4 nm diameter Pt particles catalyst suspend homogeneously with capping agent during synthesis, but without PA the catalyst particles become large agglomerates 30-40 nm in diameter. In that case, capping agent we added did play a role in "capping" the particles and preventing them from aggregation.

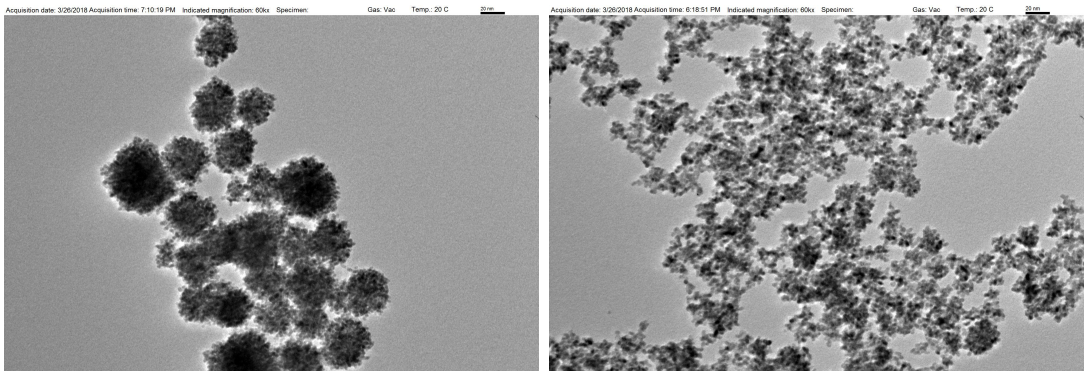

Figure 3.6: The effect of capping agent. Left: sample synthesized without capping agent, particles remain a "particle cloud" with 30-40 nm in diameter. Right: sample synthesized with capping agent. the 3-4 nm platinum nanoparticles keep homogeneous and separate even after long time from synthesis.

3.3 Electrochemical Results

3.3.1 Comparison between bulk Pt and nanoparticles

The electrochemical behavior of a bulk Pt electrode and Pt nanoparticles was first explored in 0.5M H_2SO_4 electrolyte by running cyclic voltammetry (CV) from +1.25 to -0.25 V vs Ag/AgCl. Figure 3.7 shows representative voltammograms of a smooth bulk Pt electrode and decontaminated nanoparticles.

Both voltammograms show the typical current-potential behavior for platinum corresponding to forming and breaking bonds of Pt–H and Pt–O. Hydrogen adsorption is observed when the scan goes from positive to negative, starting from 0 V vs. Ag/AgCl, and corresponding desorption starting from negative to positive. Oxygen adsorption waves appear at +0.9 V and above, with corresponding desorption in the reverse scan occurring at +0.4 V. The nanoparticle plot has the same peaks shape as bulk platinum one, clearly indicating platinum particles on the electrode. However, the peaks are not as sharp or clear for the nanoparticles compared to bulk Pt, indicating that probably our particles after decontami-

nation are not clean enough, or the particles could have changed their surface composition after the electrochemical cleaning process. The Pt nanoparticle data also has much larger peaks, which agree with our assumption that particles have much larger surface area than the Pt button. We concluded that our particles were not clean enough, and a series of different electrochemical cleaning methods are discussed in the next subsection.

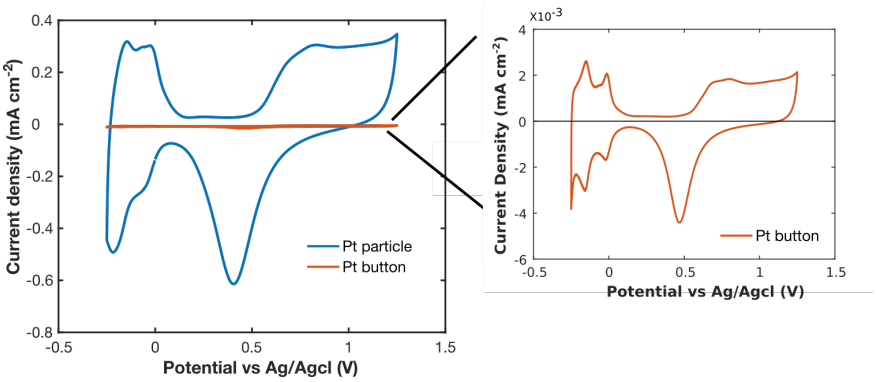

Figure 3.7: CV plot shows the shape of clean platinum nanoparticles and higher current density than platinum button electrode. High current in CV plot means more active sites of catalysts. The blue curve is for nanoparticles and red and yellow (coming together) are for the platinum bulk catalyst before and after the nanoparticles CV cycles

3.3.2 Electrochemical cleaning

Polyacrylate capping agent works effectively in preventing nanoparticles from growing and attaching to each other in synthesis. However, it is also necessary to remove the capping agent after synthesis in order to expose the Pt surface to reaction. Different methods have been tried for removing the capping agents by different groups: Park et al. pointed out that the organic capping agents on Pt nanoparticles can be decomposed by UV/ozone treatment[42]. They verified the capping agent removal by ethylene hydrogenation and showed the decrease in the distance between particles after the UV treatment[43]. Solla-Gullon et al. found out that Pt nanoparticles could be cleaned electrochemically besides those methods mentioned above. [44, 45] They also verified that the crystal structure of nanoparticles would not be modified after electrochemical cleaning [33].

In our experiment, the electrochemical cleaning method was chosen because compared to other methods, this one didn't need extra technique or complicated reaction condition. The electrochemical cleaning was done under exactly the same reaction atmosphere with adsorption/desorption CV plots, and the decontamination process could be done by enlarging the potential limits to a broader range during CV experiments. This method is also known as a "classic electrochemical activation" of Pt electrodes. For example, we usually set the potential between -0.25–1.25V vs Ag/AgCl to see the peaks of adsorption and desorption of hydrogen and oxygen on the Pt surface. But for the cleaning procedure, we switched the scan limits to -0.4–1.5 V vs Ag/AgCl and let some of the oxidation and evolution happen at the platinum surface. The reason that this cleaning method is, as Solla-Gullon et al. pointed out, gets rid of the ions attached to the Pt surface by oxidation in turn releasing gas. This attachment also enabled contaminates to fall off from the catalyst surface, so that the catalyst has more clean area after this cleaning procedure.

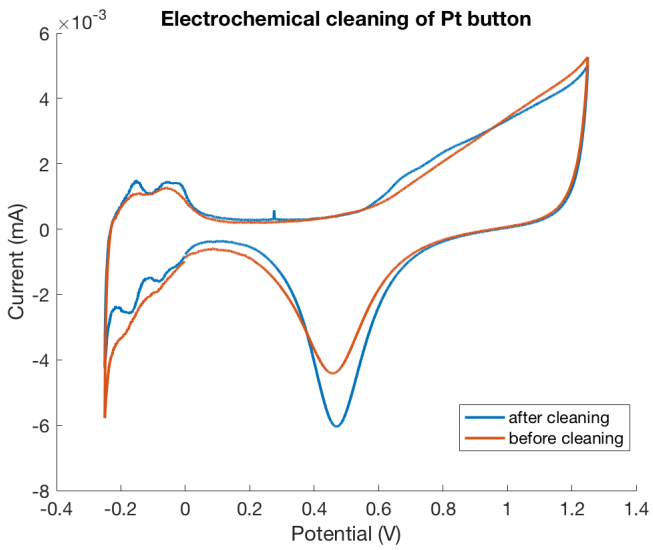

Figure 3.8: CV plots of Pt button catalyst before and after electrochemical cleaning method. Note the potential shown in the figure is versus Ag/AgCl.

Both platinum button and nanoparticles need cleaning before measurement, because platinum is very reactive, even at room temperature in air platinum will react with oxygen and become platinum oxides. Platinum oxide is a much worse catalyst for electrochemical application than pure platinum, and the oxide on the surface block platinum active surface as a contaminant. Figure 3.8 shows the Pt button plot before and after cleaning step. It can be seen that after electrochemical cleaning, the adsorption and desorption peaks for Pt button become more apparent.

For Pt nanoparticles, the electrochemical cleaning gives a more effective result than with a button, as shown in Figure 3.9. Multiple cycles were run to collect the data throughout the cleaning process. It is interesting to see that as the cycles increase, the current grows larger and the peaks come out. This peak-growing process means that there are more hydrogen and oxygen reacting with platinum atoms with cycling—that is to say the catalysts are becoming cleaner and this binding and breaking process is acting as the cleaning procedure itself. This conclusion corresponds to prior work showing that running more cycles of hydrogen/oxygen adsorption and desorption could have the same effect as the classical electrochemical cleaning

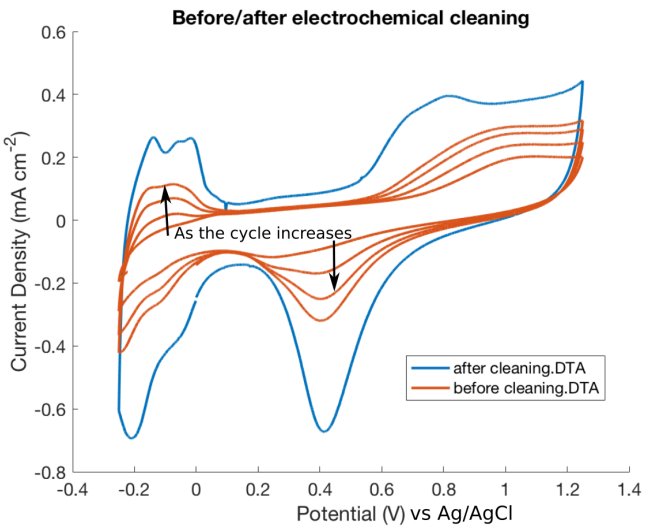

Figure 3.9: Pt nanoparticle catalysts CV before and after electrochemical cleaning.

[44]. The reason why nanoparticle peaks change more than the button peaks is consistent with a difference in surface area. The surface area of the button is very small compared to nanoparticles even though the amount of suspension deposited on the electrode is small. Meanwhile, for button electrodes the contaminant can only attach to the outer layer, but for nanocatalysts every particle could be contaminated by capping agent and once it is removed the total active area is significantly increased after the cleaning procedure.

To summarize, the results above indicated that there was some contaminant remaining on the surface of Pt after base treatment, but they could be removed from catalyst surface by electrochemical cleaning procedure, which lead to typical hydrogen binding and breaking peaks at Pt metal.

3.4 Quantitative Measurements

Catalytic mechanisms in electrochemistry are analogous to gas-phase processes in that they involve binding of the reactant molecule to the catalyst surface. The reason why nanocat-

alysts are better than bulk ones is because they provide larger total surface areas, enabling more reactants to bind at the same time. It is important to know the actual catalyst surface area to assess how effective they are. We also expect that comparing theoretical surface areas and actual ones will help us understand whether the particles have been adequately cleaned of contaminants and capping agent. Instead of directly measuring the area of Pt nanoparticles synthesized, another method was used to measure the active surface area using electrochemical experiments, as described below.

3.4.1 Electrochemical surface area

As nanomaterials are gaining more and more interest in catalysis field, many methods have been introduced to measure the surface area of nanoparticles. For example, one group used an electrical aerosol detector (EAD) for nearly spherical nanoparticles surface area measurement [46]. Another group determined the surface area using CO stripping measurements [44, 47]. These researchers pointed out that the CO stripping could be used as a cleaning method for Pt nanoparticles as well. We chose the well-established electrochemical surface area [48] (ECSA) method to determine the active surface areas of particles, as illustrated in figure 3.10.

The number of sites that can form hydrogen bonds is measured electrochemically and used to calculate active surface area of the nanoparticle film. Several assumptions are made here, such as there is no deposition after the desorption, meaning the number of Pt–H bonds broken will be the same as number of bonds formed, so that the catalyst site is still active after the adsorption and desorption of hydrogen.

The ECSA method is based on the following equations:

$$\mathbf{Q}\ (\text{hydrogen adsorption charge, mA·S}) = \frac{\int \text{idv (mA·mV)}}{\text{scan rate(mV/s)}} \tag{3.1}$$

$$\text{ECSA (cm}^2) = \frac{\text{adsorption charge Q (μC)}}{210\text{μC/cm}^2} \tag{3.2}$$

Q (μC) represents the total charge in the adsorption process. Because one proton binds to the Pt surface, inducing one electron transfer, we can take the electron transfer charge

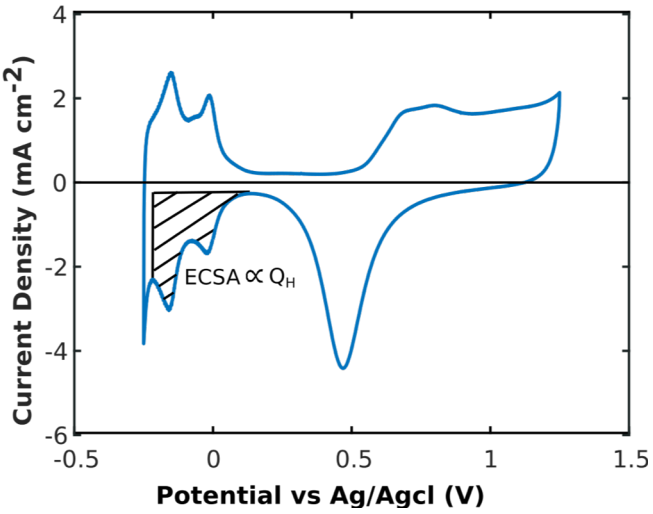

Figure 3.10: The electrichemical surface area of hydrogen evolution can be calculated by the shaded area in figure.

as the number of H atoms binding on the Pt surface. Q is thus the integral of the observed current density in the shaded area, and 210μC is the standard adsorption charge density of 1 layer of H on 1 square cm of Pt. By dividing the actual adsorption charge by the standard charge density, we can determine how many square cm of Pt catalyst surface is on the electrode—the electrochemical surface area (ECSA).

3.4.2 Theoretical area calculation

The theoretical particle surface area shows how much surface area that should be exposed in the reaction. By calculating this and comparing with electrochemical surface area, we are able to tell if our nanoparticles are clean enough after the purification methods. Theoretical surface area is calculated based on the nanoparticle size from TEM results. Particle shape is simplified by assuming perfect sphere. The diameter of each particle is averaged by picking up 50 particles randomly in TEM image. For each particle, the long and short axis are both measured and are averaged. The volume of a single sphere particle can be calculated after we know the diameter, also the mass of a particle is known by multiplying by the density of

platinum. Dividing the whole theoretical mass by single particle mass we can get the number of particles in the sample and finally the total surface area can be calculated by multiplying the number of particles and single particle surface area together. Finally, according to the particle size and mass, we calculated the surface area of a single particle and then the total theoretical surface area. Yield was calculated dividing ECSA result by theoretical surface area, and the results were shown in table 3.2.

Note that theoretical catalysts surface area calculation is based on several assumptions. First, we approximated the geometry of the nanoparticles as spheres, where the long and short axis of each particle were measured using software and averaged to be the diameter of the sphere (as shown in the below part of figure 3.11). Second, each nanoparticle is assumed to be separate from the others, meaning there is no aggregation. Third, the 50 particles we picked up were used to represent all the particles size to approximate the average mass of a single particle.

There are some shortcomings of this method, which could affect the comparison of those surface areas and even lead to the inaccurate conclusion whether our particles are clean enough. First, for theoretical surface areas, the sizes of platinum nanoparticles were estimated using 50 randomly selected particles and assuming they were perfect spheres that were not in contact with each other, meaning that the entire area should be active if they were successfully cleaned. However, from the TEM images we can see that not all of the particles are spheres—some of them appear to be square, some spheroidal with a long axis, and some are hexagonal. The particles are also clearly somewhat aggregated. Weak aggregation is not significant, because the blocked area only accounts for a very small part of the whole particle area; but if some of the particles fully fuse, the area would be significantly different from what we assume. As TEM only gives us 2D images, we cannot tell if the particles are simply overlapping or fusing together during the reaction or centrifugation. To summarize, using these methods to estimate and compare the surface area of nanoparticles does have some limitations, but they still give us an indication of whether our catalysts are clean and therefore help explain how they perform in electrochemical experiments.

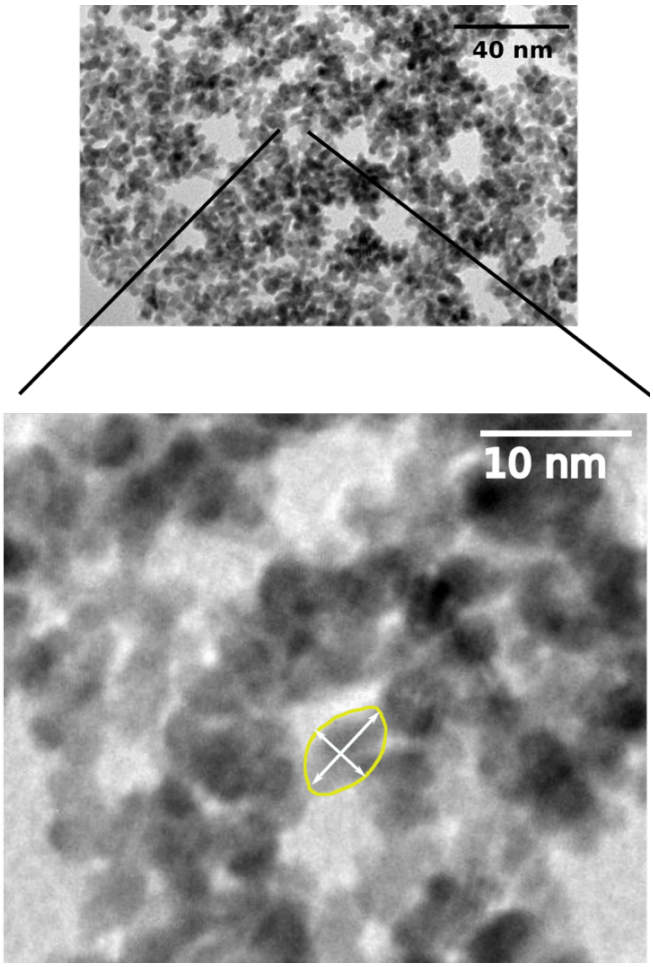

Figure 3.11: The theoretical area can be calculated by selecting a part of TEM image as example.

Table 3.2: Theoretical and actual surface area calculation

Average diameter	3.718 nm
Single particle volume	26.911 nm^3
Pt density	$2.145*10^{-17}$ mg/nm^3
Single particle mass	$5.772*10^{-16}$ mg
theoretical total mass	1.95mg
Particle number	$3.378*10^{15}$
Single particle surface area	43.427 nm^2
Total surface area (Theoretical)	1466.96 cm^2
Total surface area (Actual)	277.18 cm^2
Percentage (actual/theoretical)	18.9

3.5 Particle Treatment Methods

3.5.1 The influence of base concentration

A sodium hydroxide pellet is added to the sample after synthesis to remove the capping agent, polyacrylate (PA). However, it is unclear exactly how much base should be added to remove the PA completely. Several base concentration were therefore tried by changing the mass added to the sample to find out the appropriate concentration. The cleanliness of particles were then tested using cyclic voltammetry. Qualitative results are shown in Figure 3.12.

Different concentration for samples were chosen based on previously reported procedures [44, 45]. Particles were left to settle for at least 24 hours. We found that for NaOH concentrations of 0.3M and higher, the particles behaved similar— 0.3M base was enough to cause particles to separate from the supernatant successfully.

Figure 3.13 shows the corresponding electrochemical results. The peaks in the cyclic voltammetry plot reflect the bonds formed on the metal. Larger and clearer peaks indicate that the catalyst has been more completely cleaned.

The sample with no base treatment gave no clear peaks for formation and breakage of Pt–H and Pt–O bonds. This agrees with our expectations because if no base is added to the sample, the Pt particles remain covered with capping agent and no active surface will

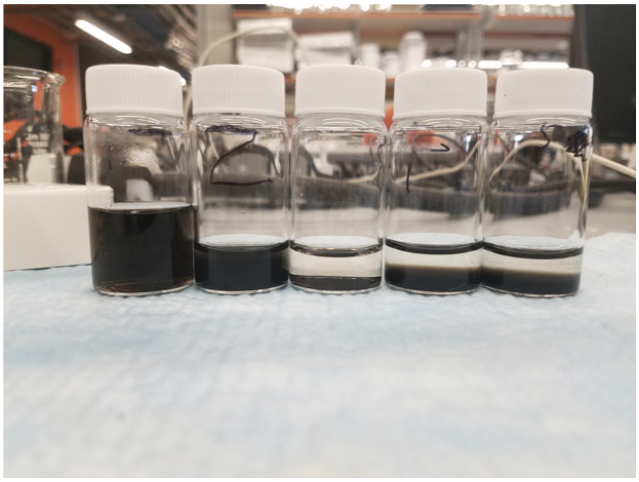

Figure 3.12: left to right: samples with no base, 0.175M, 0.35M,0.7M, 1.0M NaOH treatment after 24 hours.

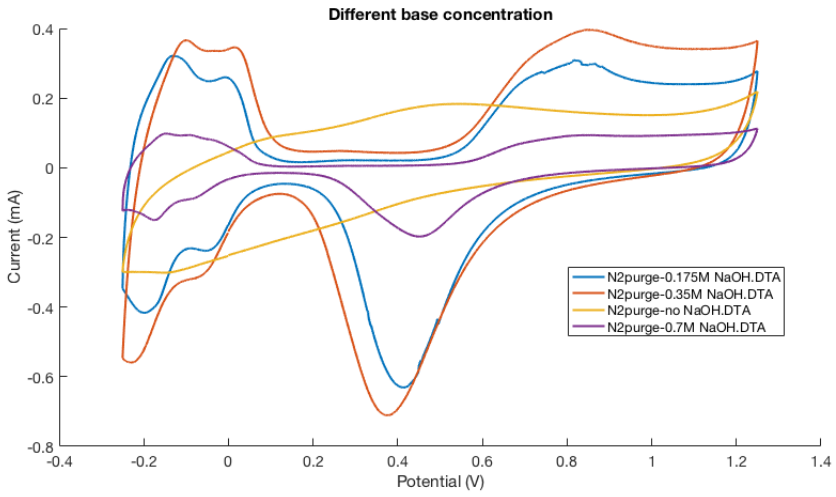

Figure 3.13: The CV plot of samples after different concentration base treatment, the effect of different concentrations of NaOH is illustrated in the plot.

be exposed to the reaction. Looking at the rest of the data, the peaks became higher as the concentration increased to 0.35M, but when the concentration further increased to 0.7M the peaks became much lower and flatter in shape. Thus, we adopted a 0.4M base treatment over 24 hours to clean our nanoparticles.

3.5.2 Influence of scan rate

Figure 3.14 shows CVs of a Pt nanoparticle electrode over scan rates from 10 mV/s to 500 mV/s. Ideally, in a very accurate experimental condition, the adsorption and desorption peaks will increase linearly with scan rate, so that the ECSA result will be the same for different scan rates. However, as shown in Figure 3.15, we can see that when the scan rate was around 100 mV/s, the adsorption charge or ECSA was the largest. We therefore considered what could be the reason for the ECSA difference when applying different scan rates. We concluded that the low and high scan rate data both underestimated the true ECSA, as described below.

When the scan rate increases, hydrogen adsorption starts later and ends later. This means the entire hydrogen adsorption peaks will shift outward. But in our experiment, we set the scan limit to be the same for every scan rate in order to change only one parameter. This may lead to some part of the large scan data cut off by not going to negative enough potentials to expose the whole adsorption peak.

On the other hand, low scan rates also result in smaller apparent ECSA values. There are contaminants in electrolyte such as polyacrylate that were removed from electrode surface during the cleaning procedure prior to the CV measurement, or side products from the sample that were not washed away by purification step. During the measurement, contaminants tend to get to the surface of electrodes and block the active site. The voltammograms take longer time for each cycle measurement as the scan rate decreases, giving more time for contaminants in the solution to diffuse to the electrode. That's the reason why lower scan rate could also lead to a lower active surface area. After multiple repetitions, our experimental data suggest that 100mV/s scan rate led to the largest ECSA result, which we consider to be nearest to the correct value.

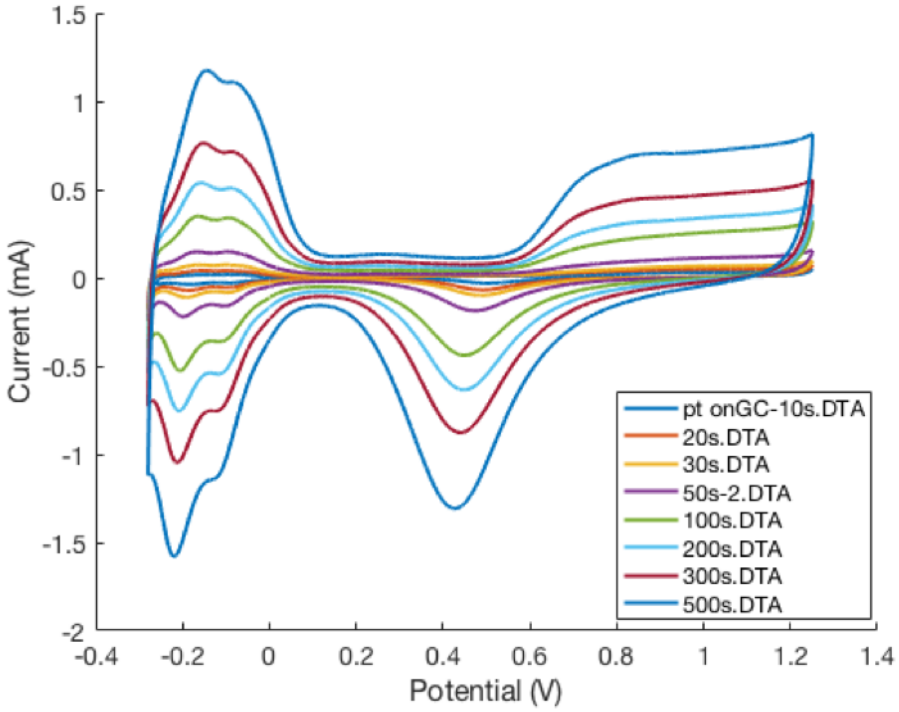

Figure 3.14: Different scan rates lead to different ECSA result for a single electrode.

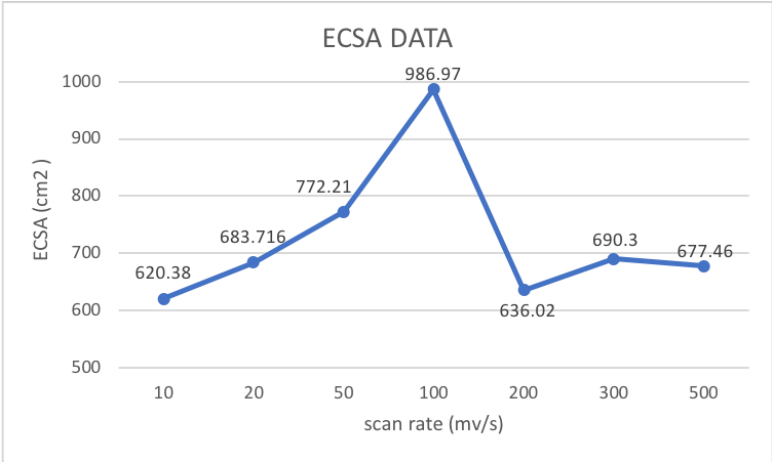

Figure 3.15: ECSA data at different scan rates

3.5.3 Stirring speed effect

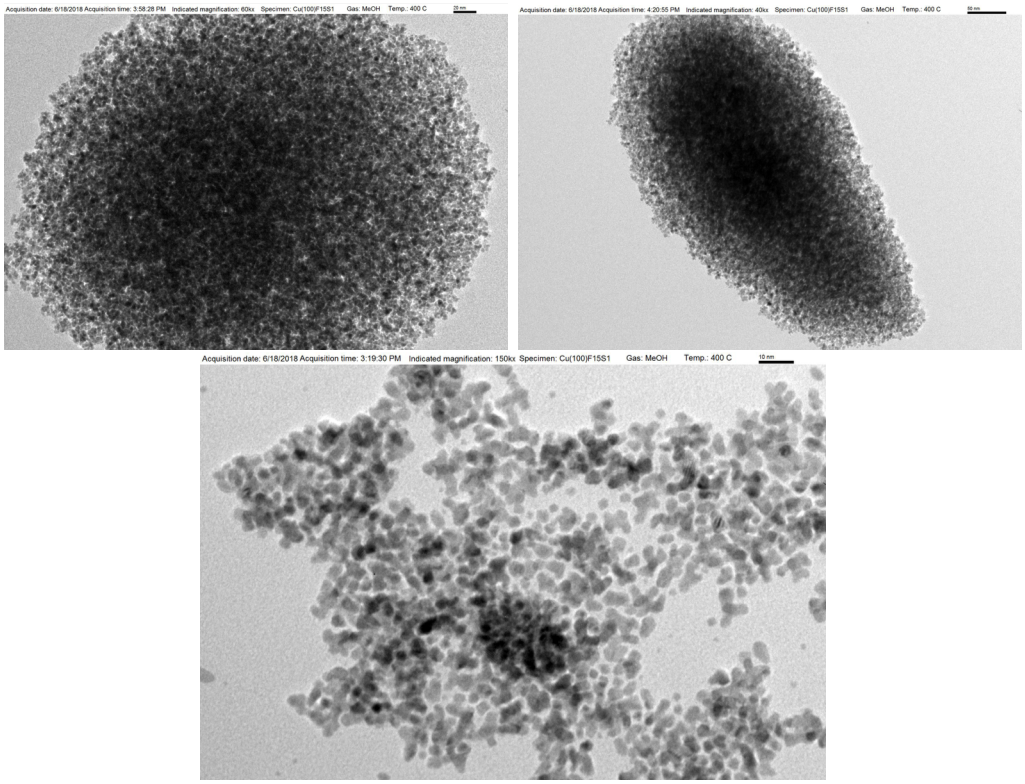

Figure 3.16: TEM images show a lot of difference in the aggregation morphology of platinum particles after various stirring conditions; Above: platinum sample synthesized under no stirring speed. Below: platinum nanoparticles synthesized under 600 rpm speed

In the synthesis process, the stirring speed is of interest in understanding the nucleation and growth of Pt nanoparticles. Kaner, et al.[49] reported that stirring may help with two things: separating the particles in the solution and maintaining uniform concentration in the reactor. The shear introduced may also increase the chance of collision of particles in both intensity and probability. Each of these processes may have an effect on particle growth and aggregation, as described below.

Kaner noted that there are two types of nucleation mechanisms for nanoparticles – homogeneous nucleation and heterogeneous nucleation[49]. In homogeneous nucleation, the nuclei grow simultaneously in the parent phase when the concentration of the reactor reaches a threshold level of super-saturation. In this case, stirring may disrupt nucleation by de-

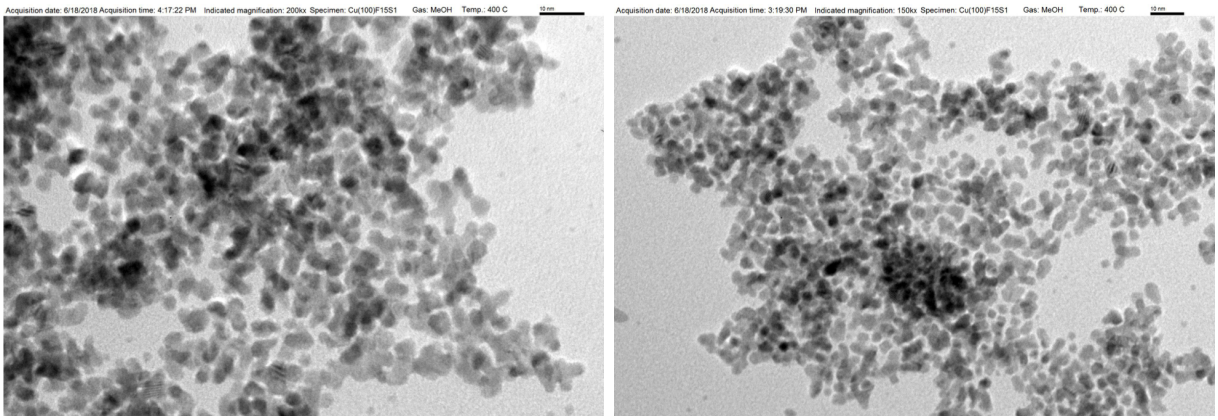

Figure 3.17: Zoom in pictures from the images above. Above: 0 rpm sample; Below: 600 rpm sample. The scale bar are 10 nm for both images.

creasing the local concentration. However, heterogeneous nucleation can be enhanced by increasing the chance of particle collisions and lowering the activation energy for growth. In this case, the new nuclei form on the existing particles and act as a "glue" or "bridge", forming larger particles overall. This means heterogeneous nucleation also favors particle aggregation or fusing. Kaner's work also included simulations suggesting the stirring shear will facilitate the heterogeneous nucleation, therefore leading to the agglomeration of particles.

To assess the effect of stirring in our system, three synthesis procedures were carried out while controlling the stirring speed to be 0, 60, 600 rpm (otherwise identical to the procedure described in the Experimental section). Interestingly, the TEM images shown in Figure 3.16 gave almost the opposite conclusion from Kaner's result—the no-stirring sample showed very strong aggregation of particles while the 600rpm-stirring sample had comparatively well-dispersed particles.

However, upon zooming in on the edge of the large agglomerate, the particles arrangement are quite similar for the 0 rpm sample and the 600 rpm sample, as shown in Figure 3.17.

By comparing our figures, it is easy to realize that stirring seemed to decrease the extent of agglomeration at the large scale, and did not seem to result in increased fusing or aggregation of particles. The reason for the phenomenon could be the stirring mainly

acts to create a uniform concentration during synthesis, and does not substantially enhance nucleation through particle collision. Kaner's work suggested stirring would facilitate the heterogeneous nucleation. From our results it can be inferred that our synthesis is dominated by homogeneous nucleation, so that stirring at this rate does not introduce enough shear to drive heterogeneous nucleation.

3.5.4 Annealing effects

Since Pt particles are interesting for many catalysis applications, we were interested to understand the effects of thermal processes on their cleanliness and performance. Several previous reports suggest that thermal annealing of Pt particles in air could be an effective way to remove the surfactant on the particles, but over-heating could lead to deleterious effects. For example, Hetper et al. pointed out that the metal polyacrylate compounds turn to metal carbonate oxides after decomposition at 420-470 °C [50]. On the other hand Chaston pointed out that higher temperature would turn Pt metal to Pt oxide, which could affect the performance of the catalyst. Moreover, at high enough temperature PtO_2 is volatile and could escape from the electrode or reactor[51]. However, Li et al. pointed out that annealing Pt nanoparticles at low temperature (around 185°C) in air was found to be effective for surface cleaning without inducing particle size and morphology changes [52]. They also verified their cleaning method by using TGA and infrared spectroscopy.

We attempted to replicate Li's experiment with our particles by dipping a gold TEM grid into the un-purified Pt nanoparticle suspension and comparing the particles morphology and catalytic performance before and after heating. The TEM images in Figure 3.18 shows how the nanoparticles looked before and after annealing at 185 °C.

From the images we can see that before heating, nanoparticles spread out homogeneously and we can still see single particles in the image, meaning that the aggregation was not severe. After 2 hours of heating at 185 °C, particles started to link together and it is quite difficult to see single nanoparticles. After 5 hours, they became large and dark spots, with many particles aggregated together. However, it is possible that although the particles grew in size, they could also be cleaner after heating—where the removal of capping agent is the

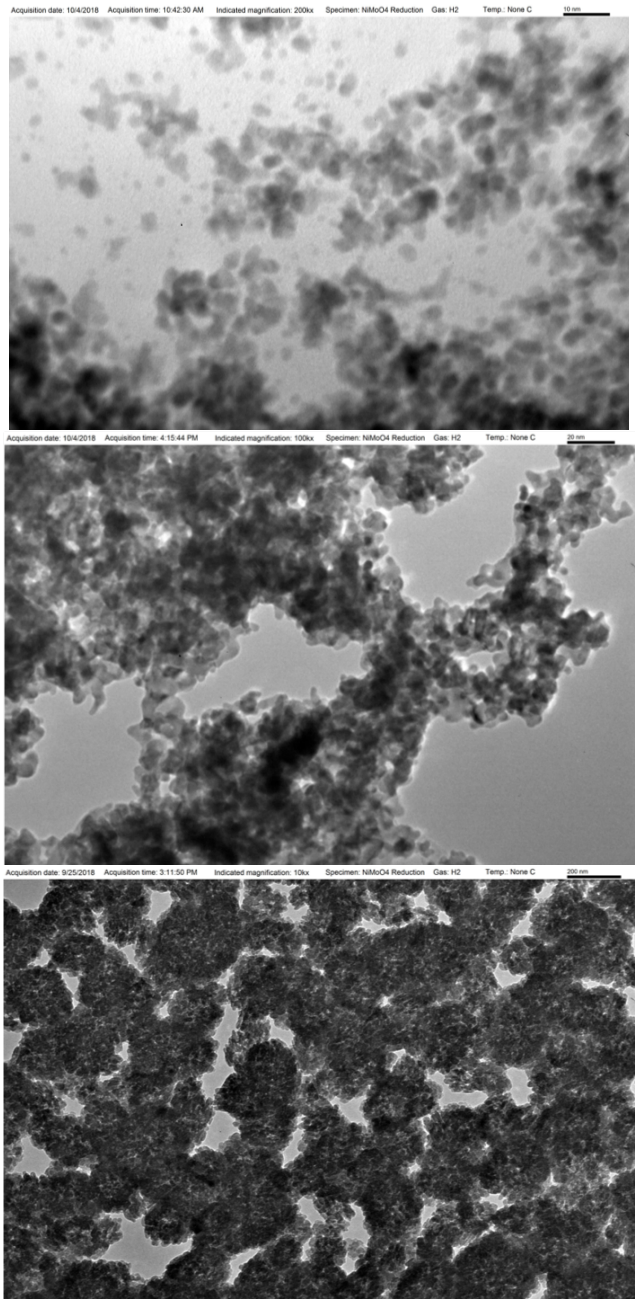

Figure 3.18: TEM images of nanocatalysts before and after annealing. Up to down: particles before annealing, after heating at 185°C for 2 hours, after heating for 5 hours.

reason for their aggregation. To determine whether aggregation or cleaner surface had a bigger effect on the nanoparticles, we measured ECSA of the Pt particles on gold TEM grids before and after heating, as shown in Figure 3.19.

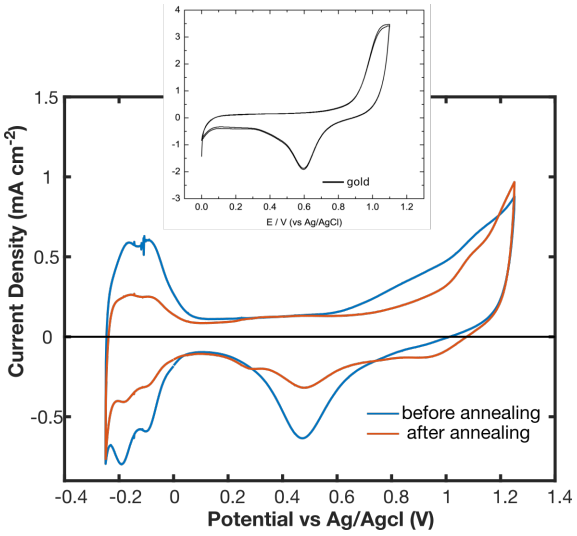

Figure 3.19: CV comparison between platinum nanoparticles before and after annealing

The results clearly show that annealing reduces the ECSA, as the size of the CV features due to hydrogen and oxygen binding was lower after annealing than before. We conclude that annealing even at high temperature is not an effective way to remove the capping agent from our particles.

3.5.5 Alternative electrochemical cleaning method

It is well established that Pt particles can be cleaned of capping agents and contaminants by running voltammograms over a wide range of applied potential. However, Topalov et al. argue that this method works by removing the surface Pt layers due to the formation and dissolution of sub-surface Pt oxides [53]. Specifically, the reduction of Pt-oxide causes the top layer of catalyst to dissolve into the electrolyte. These researchers quantified this form of Pt dissolution by measuring the Pt concentration in the solution and found that the dissolution was about 10 ng/cm^2/cycle when the positive scan limit was 1.8V vs RHE, which corresponds to about 2.4% of a monolayer per cycle.

Another consequence of electrochemical cleaning is disruption of the Pt crystal structure [54]. As a result, some other cleaning method needs to be found as a substitute for this traditional method. Solla-Gullon pointed out that using a much smaller scan limit from 0.2–1.0V vs RHE, and running many CV cycles at 500mV/s could be used as an alternative electrochemical cleaning method that has a smaller effect on the particles [33]. They verified their method by running CV for 1 hour continuously. In the first cycle they find no peak of binding and breaking, but after running for 1 hour the particles showed typical peak of clean Pt.

We attempted to reproduce the gentler CV-based cleaning method by cycling between -0.25 and 0.8 V vs Ag/AgCl, but our results (Figure 3.20, upper left) were quite different.

As shown in the results (arrows in every plot were pointing from first cycle to the last cycle), over many cycles of scanning the Pt–H adsorption peaks in fact decreased, suggesting a decrease in active surface area or loss of particle mass during cycling.

As Kneer et al. pointed out[55] the decrease of the current density could be due to cathodic dissolution, or it could be due to progressive adsorption of contaminants that are stable in this potential range. We adjusted the experiment by increasing the scan rate to reduce the time for reaction with so many cycles, and decreasing the voltage from 0.8V to 0.2V vs Ag/AgCl gradually in order to eliminate the effect of oxygen reaction and sub-layer formation. From figure 3.20 (upper right and lower panels), we can see that even after we remove the whole oxidation scan limit the peaks are still shrinking during the process. The lower panels also show an obvious shift of peak position, which suggests a change in crystal structure, or surface exposure for the platinum particles. Another possible reason for this phenomenon is that some impurities remained in the electrolyte, which would block specific Pt surface sites.

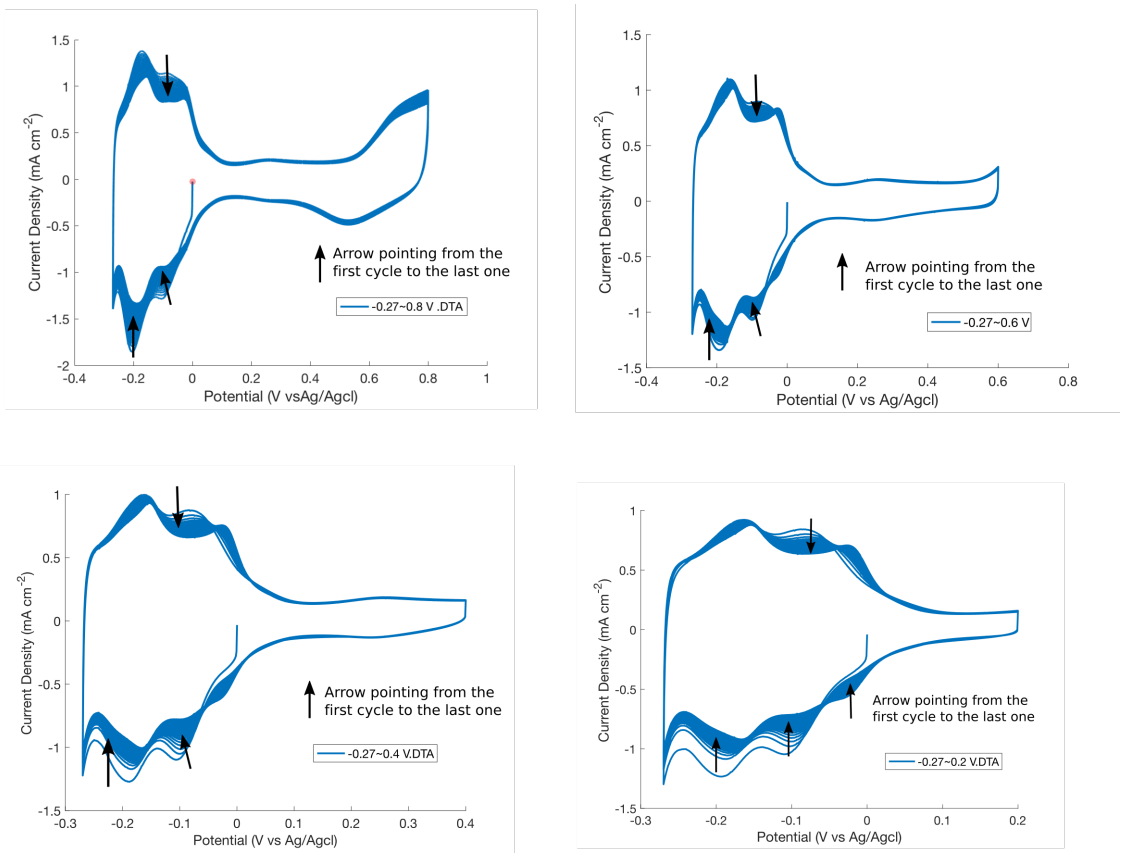

Figure 3.20: Cleaning method with running many cycles. The scan limits are shown in each figure

3.5.6 Discussion of particle cleaning methods

We attempted various cleaning procedures based on previous results. The effect of those cleaning methods was studied using CV to compare electrochemical-active surface area. For several procedures, we got different results than others, but some methods were found to work well in cleaning our particles. The best cleaning method for the Pt particles that I synthesized can be described as follows.

1. Treat the synthesized particles in 0.4M base for over 24 hours until all the particles settle down and separate from the supernatant.

2. Deposit the catalyst particles onto a glassy carbon electrode from a water suspension.

3. Cycle the electrode using CV between -0.13 and 1.13V potential vs RHE at 100mV/s scan rate before the actual catalysis application.

Although this method is still limited by the dissolution of platinum into the electrolyte and removal of outlayer catalyst by the sub-layer oxide, this method is quite reproducible and will give the cleanest apparent Pt surfaces.

3.6 Comparison with commercial Pt catalysts

In order to know if our nanocatalysts are clean enough after several cleaning treatments, a comparison with a sample of commercial platinum catalyst with a clean surface was conducted. Both of them were put in the same reaction atmosphere in CV to see the hydrogen peaks and then ECSA was calculated. ECSA were calculated respectively to see the surface area exposure of these 2 samples. 2 samples beginning with the same total concentration of Pt (2mg/mL) were cycled in exactly the same electrolyte and had the same loading of catalysts on glassy carbon electrodes. From the CV peaks in figure 3.21 it is apparent that the peaks for the commercial sample are larger than our sample.

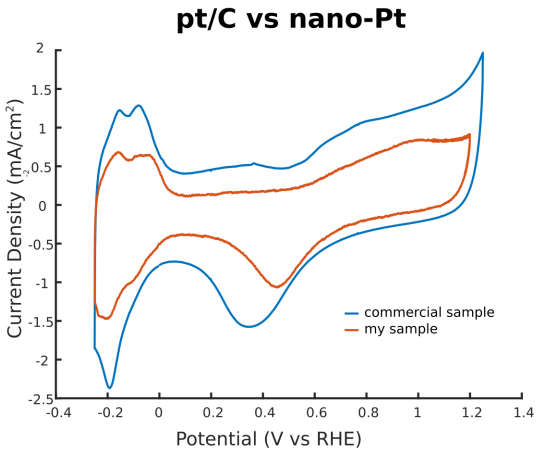

Figure 3.21: Comparison between our sample with commercial Pt/C catalysts in CV plots

However, this does not necessarily mean that the commercial sample has more surface area than our sample. The commercial Pt catalyst is supported on carbon, so it has larger double layer capacitance (the flat region of the CV is wider), but the double layer capacitance doesn't contribute to the hydrogen absorption and desorption. This double-layer capacitance needs to be subtracted before surface area comparison. The result for ECSA of 2 samples is shown in table 3.3.

From this result, it can be seen that our sample has approximately 85% of surface area of the commercial catalyst, which is a promising result because it means our particles are relatively clean after the treatments mentioned above. TEM images of these 2 samples in figure 3.22 also show that the commercial sample nanoparticles are a little bit smaller than our sample, which may be another reason for a larger surface area for the commercial sample with the same mass of platinum. However, it is surprising that even the commercial sample, which has similar particle size with our sample, with clean platinum surfaces only account for 20% of the theoretical area we calculated for our particles. . This result suggests substantial inaccuracies for our theoretical area calculation, or a systmatic under-estimation of the ECSA relative to the total Pt surface area. This could again be related to the level of cleanliness of our reaction environment.

Table 3.3: Comparison of active surface area by ECSA between our sample and commercial sample

Sample Name	ECSA (cm^2)
Commercial sample	281
Our sample	239
Ratio	0.85

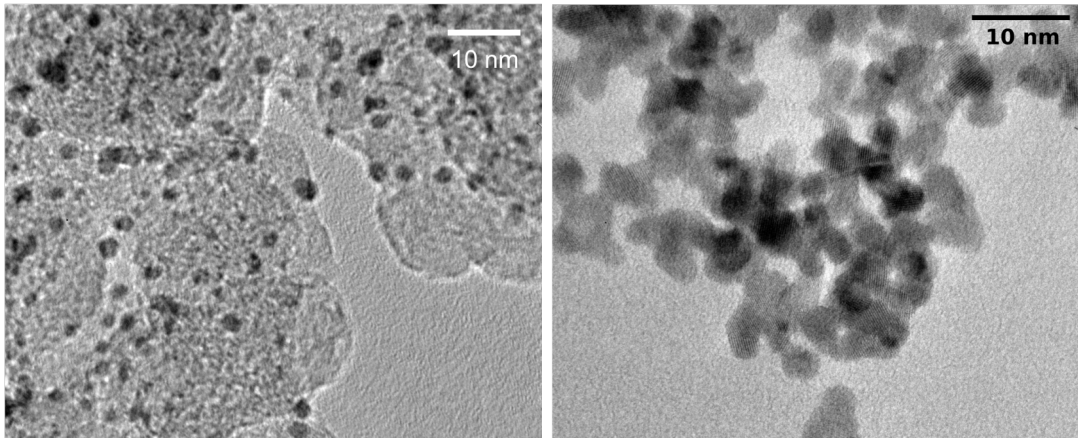

Figure 3.22: TEM images clearly show the size difference of the 2 samples. left: commercial platinum on carbon substrate, with 2.405 nm average diameter. right: platinum nanoparticles without substrate, with 3.718 nm diameter after averaging from 50 particles.

4.0 Hydrogen evolution and oxidation (HER & HOR)

4.1 Open-Circuit Potential Measurements

All of our cyclic voltammetry data used Ag/AgCl as the reference electrode, but the more commonly accepted reference electrode in hydrogen evolution is the reversible hydrogen electrode (RHE). Using RHE it is easier to analyze the data taken in hydrogen evolution experiment, because it sets the equilibrium potential of the reaction to 0 V. Therefore, the overpotential for the hydrogen evolution reaction is the absolute value of the applied potential referenced to RHE. So it is very important to be able to accurately convert a potential collected with reference to Ag/AgCl to the RHE scale. One way to convert potentials recorded using one reference electrode into potentials reported versus another reference electrode is to use a set of equations based on theoretical equilibria from tabulated values. For example the conversion from Ag/AgCl to RHE in a typical supporting electrolyte at room temperature can be done with equation 4.1:

$$E_{RHE} = E_{Ag/AgCl} + 0.059 * pH + E^0_{Ag/AgCl} \tag{4.1}$$

Where $E^0_{Ag/Agcl} = 0.198V$. However, this method can still give an incorrect calibration because the actual potential of the reference electrode depends on its precise composition as well as that of the electrolyte. So it is risky to simply shift CV data recorded with the Ag/AgCl electrode using these methods.

A better and more accurate method is to directly measure the reference potential in the experimental setup. This can be done for measuring RHE by using Pt electrode to "sense" the equilibrium potential of hydrogen evolution/oxidation. In this way, the conversion can be easily made by using equation 4.2:

$$vsAg/AgCl + OCP = vsRHE \tag{4.2}$$

Where OCP is the open-circuit potential of a clean Pt electrode in the electrolyte when it has been saturated with 1 atm of H_2 overpressure. It is worth noting why we do not use the same Pt electrode directly as reference. The main reason is that solid reference electrodes like Ag/AgCl are much more stable over long periods of time than Pt-based RHE references. This makes them easier to use as long as we do a proper calibration.

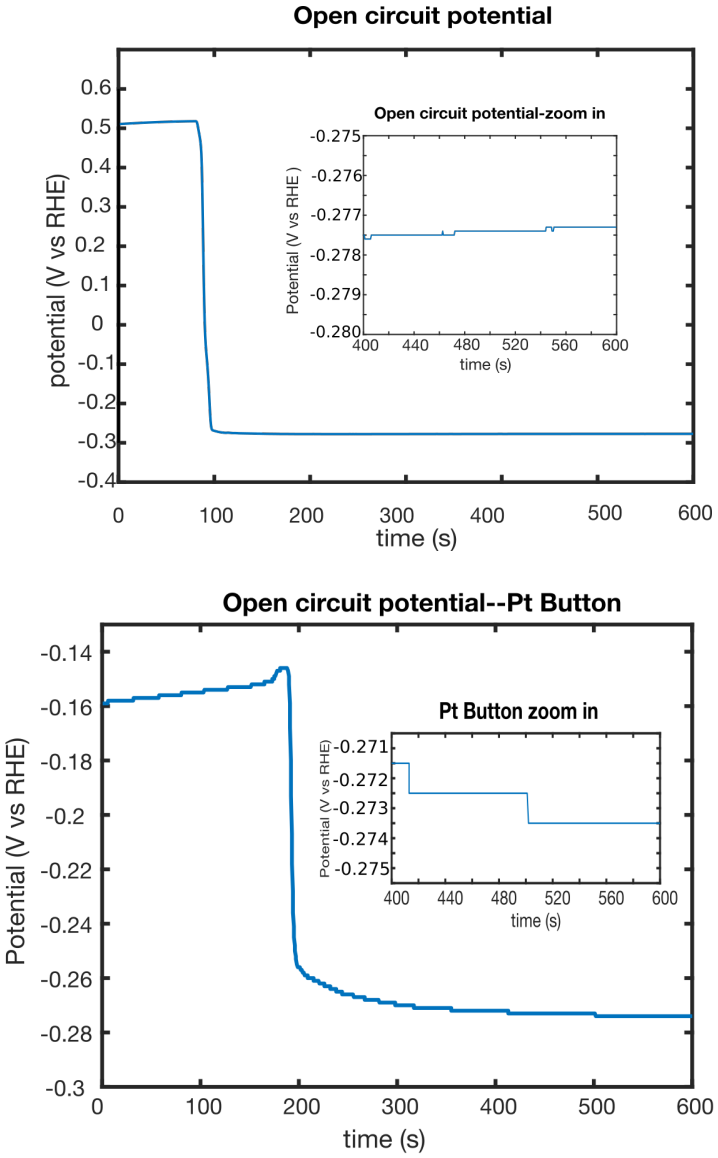

Figure 4.1: The open circuit potential of reference electrode driven by platinum nanocatalysts is very stable compared to Pt button electrode. Above: nanoparticle OCP. Below: Pt button OCP

RHE experiments for both button and nanoparticles were done using the same 3 electrode setup as CV measurement. 0.5M sulfuric acid electrolyte was freshly made every time and exposed to air when the experiment began, then after the potential were stable for a while, hydrogen was purged into the electrolyte and potential reduced very fast in several seconds, as shown in figure 4.1. After around 30 seconds of hydrogen purge, the electrolyte was gradually saturated with hydrogen and the potential value became stable, and remained stable for a long time. If the change of potential was within 5mV in 120 seconds, the potential value was written down as the open circuit potential of reference electrode in this reaction atmosphere. Note that hydrogen was continuously purged during the experiment to ensure a stable reaction atmosphere in the whole measurement. Figure 4.1 shows OCP results for both Pt button and nanoparticles under the same circumstance. It can be seen from comparison that OCP with nanoparticles had less noise than the one with Pt button as working electrode. From the zoom in inset of those plots we also can see within the last 200 seconds in the whole measuring process, potential changed was 2mV with the button electrode, but less than 0.5mV with nanoparticle electrode. This result can be described as with nanocatalysts the open circuit potential reached its stability faster than with button catalysts, indicating nanoparticles can catalyze the open circuit potential reaction faster than button catalyst. The reason for this phenomenon was quite obvious: nanoparticles had much more surface area than button catalyst so that the reaction could happen smoother and reached stability in a shorter time.

4.2 Hydrogen Evolution/Oxidation Kinetics

To assess the catalytic performance of our nanoparticles, the hydrogen evolution reaction (HER) oxidation reaction(HOR) experiment was operated with a Pt nanoparticle elecrode in acidic electrolyte. Pt is known to be able to generate large cathodic current densities for the HER at low overpotentials [56]. We varied several parameters, such as scan rate and rotation speed of working electrode in RDE system to see what effect they will bring to the hydrogen evolution performance. Figure 4.2 shows the electrocatalytic activity of the Pt nanoparticles

in 0.5M H_2SO_4, with working electrode prepared by deposition of Pt particles at a mass loading of $5.46*10^{-3}$ mg/cm^2 onto a 0.196 cm^2 glassy carbon rotating disk electrode.

From a comparison of the data, we can see the smaller scan rate makes the HER response more noisy. This is easy to explain because smaller scan rate requires longer time in the experiment. The source of noise in the experiment is mainly H_2 gas bubbles that grow on the surface of the electrode and prevent protons from coming to the surface of the electrode. The reaction then becomes transport limited rather than kinetics limited.

The lower two panels of Figure 4.2 plot the HER data collected at 50 mV/s scan rate and several different electrode rotation rate into into Tafel plot, where the x-axis is potential but the y-axis the log of absolute value of current density. These HER plots have a V-shape, where the left side is HER current and the right side is HOR current. We found that the rotation speed had a small but noticeable effect on OCP results, where the tips of all the V shape plots (which corresponds to the OCP) are slightly different from one another. The lower right panel therefore corrects these Tafel plots for the true equilibrium potential by setting the OCP to 0 V vs RHE.

From figure 4.2 it can be seen that the rotation speed has little influence on the HER, but considerably more on the HOR. The reason for this is for the HER, the surface concentration of protons is large enough that it remains homogeneous for different rotation speeds (the system is now kinetically limited during HER). However, for the HOR process, the reactant is H_2 dissolved in the electrolyte. The saturation concentration of H_2 in water at room temperature at 1 atm of H_2 pressure is 1.6 mg/L (0.8 mM), which is far less than the proton ions in the electrolyte. In this case, when the rotation speed of the working electrode increases, we found that the current density at the same potential also increases. This is because the system becomes transport-limited at this small H_2 concentration. High rotation rate reduces the thickness of the diffusion layer so that we get higher current for higher rotation rate. To summerize this part, platinum nanoparticles perform well in catalyzing hydrogen evolution and oxidation reactions efficiently by having high current density in CV plots. When we transfer those reaction plots into tafel plots, it can be seen clearly that the hydrogen evolution part is kinetics limited, with the logarithm of current density growing linearly as the potential becomes more negative. But for the hydrogen oxidation part, Tafel

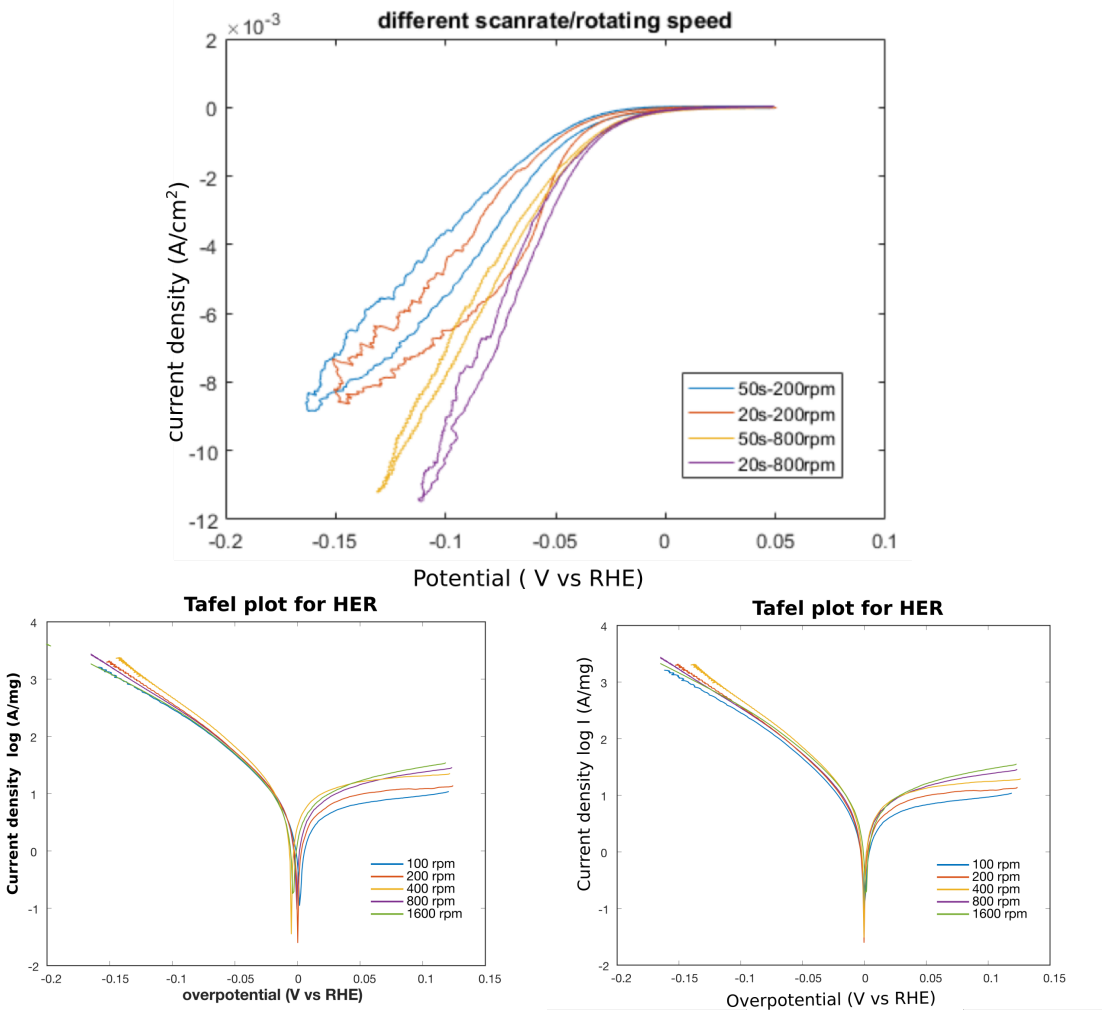

Figure 4.2: Hydrogen evolution was conducted controlling rotation speed of working electrode. The data was transferred and put in Tafel plot to easily recognize the effect of rotation speed on the current density. Above: Hydrogen evolution controlling scan rate and rotation speed. Below left: raw data before correction. Below right: after correction for open circuit potential value and put all the plot peaks together.

plots are not linear as potential grows, indicating the reaction is limited by mass transport instead of kinetics. By controlling the rotation rate of working electrode we can solve some of this problem by forcing bubbles to the side of the electrode. But the overall HOR reaction is still mass transport limited due to low concentration of hydrogen in electrolyte and the diffusion layer at the surface of the electrode.

5.0 Conclusion and Future Work

Renewable energy is likely to continue replacing conventional fuel resources, and hydrogen has high promise as a future energy carrier. Platinum, which is the most widely used catalyst for production of hydrogen, has some desirable characteristics such as being stable and very active that could act as benchmark for other alternative catalysts. We have developed a method for synthesizing, purifying, and testing nanoscale platinum electrocatalysts using a precursor platinum salt, ascorbic acid as reducing agent, and sodium polyacralate as the capping agent. The Pt nanoparticles were observed under TEM and found to be uniform and a few nanometer in diameter, and the theoretical surface area was calculated based on TEM results.

The main advance in this project was developing a way to produce clean Pt nanoparticles using simple techniques—aqueous precursors at a modest reactor temperature. Our technique requires no explosive gas such as hydrogen as the reducing agent, and no special procedures such as generating a water-in-oil emulsion. The simplicity of the cleaning method is also important, since it requires only base, alcohol solvent, and a common type of centrifuge. As a result, this procedure can be reproduced by many labs to compare the performance of any new catalyst against high-quality Pt nanoparticles.

Several cleaning methods were explored to remove the capping agent after synthesis and purify the nano-particles from the precursors and side products. Some of these methods worked well in cleaning our nanoparticles—such as base treatment and electrochemical cleaning by enlarging the scan limits in the cyclic voltammetry. However, some of the methods did not give adequate result after several attempts, such as the method of running hundreds of "soft" CV cycles and thermal annealing. The reason for disagreement between our results and others' could be due to different synthesis methods used or different sized nanoparticles. It would be worth testing several other cleaning methods in the future, including UV-ozone treatment, CO stripping or acid washing. After cleaning, the nanoparticles were applied in electrochemical experiments to calibrate the reference electrode potential and to verify their catalytic performance. The electrochemical surface area of nanoparticles was measured

based on voltammetry data and found to be similar to that of commercial carbon-supported Pt nanoparticles. Variables such as the scan rate and rotation speed of the electrode were controlled to see their effects on apparent surface area and catalytic performance.

In industrial application, the practical performance of the catalyst is crucial, so it is important to see if these particles are useful for devices. Future work about this project could involve depositing these Pt nanocatalysts onto a membrane to test their efficiency inside a fuel cell. Also, a large number of alternative catalysts that are intended to be lower in cost are being explored to replace this traditional catalyst. Therefore this catalyst could act as the benchmark for other catalysts to work towards an economically efficient catalyst.

The shape of nanoparticles is also an important concern for this project and could become a focus of future work. Platinum particles have different crystal structures and different surface could lead to different catalytic properties for hydrogen evolution/oxidation or other reactions. It would be worthwhile to study in detail the relationship between the HER activity and the quantity and characteristics of different exposed facets of Pt particles. We also found out during our electrochemical experiment that the activity of catalyst decreased with time. For example, the hydrogen evolution current peak with the same sample will become smaller when tested 2 months after synthesis compared to a fresh sample. So sample storage, or the catalytic property recovery of Pt particles could be another focus for future work.

The aforementioned suggestions could be possible steps towards the development of clean platinum nanocatalysts. I also believe that an understanding of active catalysts' properties and practices in electrochemistry, such as mechanism, synthesis, verification and so on are the most effective validation of their potential applicability in the chemical field. The exploration of a benchmark catalyst should also contribute to lab catalyst development in the future. Finally, I hope this work provides some useful ideas to anyone after me who wants to dig deeper into similar projects, and that this research will get us closer to a sustainable future with renewable energy.

BIBLIOGRAPHY

[1] Hubert A Gasteiger et al. "Activity benchmarks and requirements for Pt, Pt-alloy, and non-Pt oxygen reduction catalysts for PEMFCs". In: *Applied Catalysis B: Environmental* 56.1-2 (2005), pp. 9–35. ISSN: 0926-3373.

[2] Eric N Coker et al. "Nanostructured Pt/C electrocatalysts with high platinum dispersions through zeolite-templating". In: *Microporous and Mesoporous Materials* 101.3 (2007), pp. 440–444. ISSN: 1387-1811.

[3] Digby D Macdonald et al. *Modern Aspects of Electrochemistry, vol. 14*. 1982.

[4] K A Friedrich et al. "Model electrodes with defined mesoscopic structure". In: *Fresenius' journal of analytical chemistry* 358.1-2 (1997), pp. 163–165. ISSN: 0937-0633.

[5] T J Schmidt et al. "Characterization of high-surface-area electrocatalysts using a rotating disk electrode configuration". In: *Journal of The Electrochemical Society* 145.7 (1998), pp. 2354–2358. ISSN: 0013-4651.

[6] K Kinoshita. "Particle size effects for oxygen reduction on highly dispersed platinum in acid electrolytes". In: *Journal of The Electrochemical Society* 137.3 (1990), pp. 845–848. ISSN: 0013-4651.

[7] Kiyochika Yahikozawa et al. "Electrocatalytic properties of ultrafine platinum particles for oxidation of methanol and formic acid in aqueous solutions". In: *Electrochimica acta* 36.5-6 (1991), pp. 973–978. ISSN: 0013-4686.

[8] James Larminie, Andrew Dicks, and Maurice S McDonald. *Fuel cell systems explained*. Vol. 2. J. Wiley Chichester, UK, 2003.

[9] Leonardo Barreto, Atsutoshi Makihira, and Keywan Riahi. "The hydrogen economy in the 21st century: a sustainable development scenario". In: *International Journal of Hydrogen Energy* 28.3 (2003), pp. 267–284. ISSN: 0360-3199.

[10] Ram Ramachandran and Raghu K Menon. "An overview of industrial uses of hydrogen". In: *International Journal of Hydrogen Energy* 23.7 (1998), pp. 593–598. ISSN: 0360-3199.

[11] N Eliaz, D Eliezer, and D L Olson. "Hydrogen-assisted processing of materials". In: *Materials Science and Engineering: A* 289.1-2 (2000), pp. 41–53. ISSN: 0921-5093.

[12] S Trasatti. "Water electrolysis: who first?" In: *Journal of Electroanalytical Chemistry* 476.1 (1999), pp. 90–91. ISSN: 1572-6657.

[13] Carlos G Morales-Guio, Lucas-Alexandre Stern, and Xile Hu. "Nanostructured hydrotreating catalysts for electrochemical hydrogen evolution". In: *Chemical Society Reviews* 43.18 (2014), pp. 6555–6569.

[14] Kai Zeng and Dongke Zhang. "Recent progress in alkaline water electrolysis for hydrogen production and applications". In: *Progress in Energy and Combustion Science* 36.3 (2010), pp. 307–326. ISSN: 0360-1285.

[15] Roberto F De Souza et al. "Electrochemical hydrogen production from water electrolysis using ionic liquid as electrolytes: towards the best device". In: *Journal of Power Sources* 164.2 (2007), pp. 792–798. ISSN: 0378-7753.

[16] D Trommer et al. "Hydrogen production by steam-gasification of petroleum coke using concentrated solar power—I. Thermodynamic and kinetic analyses". In: *International Journal of Hydrogen Energy* 30.6 (2005), pp. 605–618. ISSN: 0360-3199.

[17] Keith Oldham and Jan Myland. *Fundamentals of electrochemical science*. Elsevier, 2012. ISBN: 0323139639.

[18] R L LeRoy. "Industrial water electrolysis: present and future". In: *International Journal of Hydrogen Energy* 8.6 (1983), pp. 401–417. ISSN: 0360-3199.

[19] M S Dresselhaus and I L Thomas. "Alternative energy technologies". In: *Nature* 414.6861 (2001), p. 332. ISSN: 1476-4687.

[20] N L Panwar, S C Kaushik, and Surendra Kothari. "Role of renewable energy sources in environmental protection: A review". In: *Renewable and Sustainable Energy Reviews* 15.3 (2011), pp. 1513–1524. ISSN: 1364-0321.

[21] Mukund R Patel. *Wind and solar power systems: design, analysis, and operation*. CRC press, 2005. ISBN: 142003992X.

[22] Calvin H Bartholomew and Robert J Farrauto. *Fundamentals of industrial catalytic processes*. John Wiley & Sons, 2011. ISBN: 1118209737.

[23] Frank R Hartley. *Supported metal complexes: a new generation of catalysts*. Vol. 6. Springer Science & Business Media, 2012. ISBN: 9400952473.

[24] Keisuke Nansai et al. "Global flows of critical metals necessary for low-carbon technologies: the case of neodymium, cobalt, and platinum". In: *Environmental science & technology* 48.3 (2014), pp. 1391–1400. ISSN: 0013-936X.

[25] Karl Kordesch et al. "Alkaline fuel cells applications". In: *Journal of Power Sources* 86.1-2 (2000), pp. 162–165. ISSN: 0378-7753.

[26] James C Ely et al. "Implications of platinum-group element accumulation along US roads from catalytic-converter attrition". In: *Environmental Science & Technology* 35.19 (2001), pp. 3816–3822. ISSN: 0013-936X.

[27] Jonathan H Harris et al. *Electrolytic processes employing platinum based amorphous metal alloy oxygen anodes*. Nov. 1988.

[28] Lan Yun Chang et al. "Resolving the structure of active sites on platinum catalytic nanoparticles". In: *Nano letters* 10.8 (2010), pp. 3073–3076. ISSN: 1530-6984.

[29] J P Boitiaux, J Cosyns, and F Verna. "Poisoning of hydrogenation catalysts. How to cope with this general problem?" In: *Studies in Surface Science and Catalysis*. Vol. 34. Elsevier, 1987, pp. 105–123. ISBN: 0167-2991.

[30] Christopher Batchelor-McAuley et al. "Nano-Electrochemical Detection of Hydrogen or Protons Using Palladium Nanoparticles: Distinguishing Surface and Bulk Hydrogen". In: *ChemPhysChem* 7.5 (2006), pp. 1081–1085. ISSN: 1439-4235.

[31] Y Gimeno et al. "Preparation of 100 160-nm-sized branched palladium islands with enhanced electrocatalytic properties on HOPG". In: *Chemistry of materials* 13.5 (2001), pp. 1857–1864. ISSN: 0897-4756.

[32] Claude R Henry. "Catalytic activity of supported nanometer-sized metal clusters". In: *Applied surface science* 164.1-4 (2000), pp. 252–259. ISSN: 0169-4332.

[33] J Solla-Gullon et al. "Electrochemical characterisation of platinum nanoparticles prepared by microemulsion: how to clean them without loss of crystalline surface structure". In: *Journal of Electroanalytical Chemistry* 491.1-2 (2000), pp. 69–77. ISSN: 1572-6657.

[34] Luoxin Yi et al. "One dimensional CuInS 2–ZnS heterostructured nanomaterials as low-cost and high-performance counter electrodes of dye-sensitized solar cells". In: *Energy & Environmental Science* 6.3 (2013), pp. 835–840.

[35] Zhenghang Zhao et al. "Design principles for heteroatom-doped carbon nanomaterials as highly efficient catalysts for fuel cells and metal–air batteries". In: *Advanced Materials* 27.43 (2015), pp. 6834–6840. ISSN: 0935-9648.

[36] Yun Pei Zhu et al. "Surface and interface engineering of noble-metal-free electrocatalysts for efficient energy conversion processes". In: *Accounts of chemical research* 50.4 (2017), pp. 915–923. ISSN: 0001-4842.

[37] E Kemppainen et al. "Scalability and feasibility of photoelectrochemical H 2 evolution: the ultimate limit of Pt nanoparticle as an HER catalyst". In: *Energy & Environmental Science* 8.10 (2015), pp. 2991–2999.

[38] T. S. Ahmadi et al. *Shape-Controlled Synthesis of Colloidal Platinum Nanoparticles*. 1996. DOI: 10.1126/science.272.5270.1924. URL: http://www.sciencemag.org/cgi/doi/10.1126/science.272.5270.1924.

[39] Martha Windholz et al. *The Merck index. An encyclopedia of chemicals and drugs*. 9th edition. Merck & Co., 1976. ISBN: 0911910263.

[40] S E Fayle et al. "Crosslinkage of proteins by dehydroascorbic acid and its degradation products". In: *Food Chemistry* 70.2 (2000), pp. 193–198. ISSN: 0308-8146.

[41] Yannick Garsany et al. *Experimental methods for quantifying the activity of platinum electrocatalysts for the oxygen reduction reaction*. 2010.

[42] Jeong Y Park et al. "The role of organic capping layers of platinum nanoparticles in catalytic activity of CO oxidation". In: *Catalysis letters* 129.1-2 (2009), pp. 1–6. ISSN: 1011-372X.

[43] Cesar Aliaga et al. "Sum frequency generation and catalytic reaction studies of the removal of organic capping agents from Pt nanoparticles by UV ozone treatment". In: *The Journal of Physical Chemistry C* 113.15 (2009), pp. 6150–6155. ISSN: 1932-7447.

[44] J Solla-Gullón et al. "Electrochemical characterisation of platinum–palladium nanoparticles prepared in a water-in-oil microemulsion". In: *Journal of Electroanalytical Chemistry* 554 (2003), pp. 273–284. ISSN: 1572-6657.

[45] José Solla-Gullón et al. "Surface characterization of platinum electrodes". In: *Phys. Chem. Chem. Phys.* 10.10 (2008), pp. 1359–1373. ISSN: 1463-9076. DOI: 10.1039/B709809J. URL: http://xlink.rsc.org/?DOI=B709809J.

[46] H Fissan et al. "Rationale and principle of an instrument measuring lung deposited nanoparticle surface area". In: *Nanotechnology and occupational health*. Springer, 2006, pp. 53–59.

[47] T J Schmidt et al. "Characterization of high-surface-area electrocatalysts using a rotating disk electrode configuration". In: *Journal of The Electrochemical Society* 145.7 (1998), pp. 2354–2358. ISSN: 0013-4651.

[48] Shuhui Sun et al. "A highly durable platinum nanocatalyst for proton exchange membrane fuel cells: multiarmed starlike nanowire single crystal". In: *Angewandte Chemie* 123.2 (2011), pp. 442–446. ISSN: 0044-8249.

[49] Dan Li and Richard B Kaner. "Shape and aggregation control of nanoparticles: not shaken, not stirred". In: *Journal of the American Chemical Society* 128.3 (2006), pp. 968–975. ISSN: 0002-7863.

[50] J Hetper, W Balcerowiak, and J Bereś. "Thermal decomposition of metal polyacrylates". In: *Journal of thermal analysis* 20.2 (1981), pp. 345–350. ISSN: 0022-5215.

[51] J C Chaston. "Reactions of oxygen with the platinum metals". In: *Platinum Metals Review* 9.2 (1965), pp. 51–56. ISSN: 0032-1400.

[52] Dongguo Li et al. "Surfactant removal for colloidal nanoparticles from solution synthesis: the effect on catalytic performance". In: *Acs Catalysis* 2.7 (2012), pp. 1358–1362. ISSN: 2155-5435.

[53] Angel A Topalov et al. "Dissolution of platinum: limits for the deployment of electrochemical energy conversion?" In: *Angewandte Chemie International Edition* 51.50 (2012), pp. 12613–12615. ISSN: 1433-7851.

[54] Francisco J Vidal-Iglesias et al. "Electrochemical characterization of shape-controlled Pt nanoparticles in different supporting electrolytes". In: *ACS Catalysis* 2.5 (2012), pp. 901–910. ISSN: 2155-5435.

[55] Alexander Kneer et al. “Effect of Dwell Time and Scan Rate during Voltage Cycling on Catalyst Degradation in PEM Fuel Cells”. In: *Journal of The Electrochemical Society* 165.10 (2018), F805–F812. ISSN: 0013-4651.

[56] Eric J Popczun et al. “Nanostructured nickel phosphide as an electrocatalyst for the hydrogen evolution reaction”. In: *Journal of the American Chemical Society* 135.25 (2013), pp. 9267–9270. ISSN: 0002-7863.